Assessment of drought impacts on groundwater table in the Netherlands using gridded datasets in Google Earth Engine (GEE)

GOLNAR NAEIMI
August 2021

SUPERVISORS:
Dr. ir. R. Van Der Velde
Dr. ir. C. Van Der Tol

Assessment of drought impacts on groundwater table in the Netherlands using gridded datasets in Google Earth Engine (GEE)

GOLNAR NAEIMI
Enschede, The Netherlands, August, 2021

Thesis submitted to the Faculty of Geo-Information Science and Earth Observation of the University of Twente in partial fulfilment of the requirements for the degree of Master of Science in Spatial Engineering.

SUPERVISORS:
Dr. ir. R. Van Der Velde
Dr. ir. C. Van Der Tol

THESIS ASSESSMENT BOARD:
Prof. dr. Z. Bob Su (Chair)
Dr.Ir. T.A. Groen (External Examiner, University of Twente)

ABSTRACT

Drought impacts in different regions in the world have been affected natural ecosystems and people's properties negatively. As it progresses in every region specifically, there is no universal definition for this hazard. In the Netherlands, in recent years, the drought caused damages to many stakeholders' properties, so governmental budgets were allocated to alleviate the impacts as the current drought indicator has limitations. Twente region is located in the east of the Netherlands in higher elevation areas with sandy soil material. Drainage has made the groundwater resources of the Twente more vulnerable to drought impacts. Also, this region is far from the main surface water storage, so the high-quality primary water is the groundwater.

To decrease the wickedness, this study focuses on the permanent largest grasslands in the Twente region and assesses drought impact on the groundwater using global models in Google Earth Engine (GEE). Actual climate variables of precipitation and evaporation were derived from global models' of ERA5 and GLDAS 2.1, available in Google Earth Engine (GEE). The timeseries of daily mean precipitation deficit (PD) over 20 years (2001-2021), cumulative PD, and driest year with the highest PD and lowest surplus of 2018-2019 were analyzed for the two models and KNMI data.

Daily mean values over 20 years of the models were evaluated separately with the reference data of KNMI using performance metrics of R coefficient, RMSError, and Mean Absolute Error(MAE). The precipitation ERA5 shows a stronger correlation with KNMI than the GLDAS2.1, respectively correlation coefficient R 0.683, 0.532. However, for the evaporation, especially GLDAS 2.1 indicates a very strong 0.988 and ERA5 a bit lower 0.959. The actual evaporation from the models is strongly in accordance with the reference evaporation in KNMI.

Finally, the time series of the groundwater wells from different places in the Twente region and cumulative PD (2001-2021) were analyzed using in-situ measurements data in DINOloket. The groundwater measurements and cumulative PD from ERA5 data were correlated. All three groundwater wells data show that groundwater fluctuations persistently decline (Sep2005-Dec2019). The standard anomalies derived from groundwater show that drought propagation in the region is different. For instance, the B34G0251 in the southern part where the groundwater is shallowest than two others; the groundwater table is more vulnerable to drought impacts. In the first years of the study, this well has the highest inverse correlation that responds with a lag compared to other wells to PD. It probably happened due to the natural flow direction of groundwater towards that area. Again, in the well B34G0251, anomalies near the end of the study period and some years before 2018 became more intensive, and the lowest groundwater table occurred earlier than the highest PD. The earlier response reflects non-climatic factors that caused higher anomaly intensity in this area. The results indicate that drought progressed to the shallow groundwater area in the southern part of the Twente. For future research, the possibility of artificial groundwater recharge using an annual surplus is recommended to prevent more progress of drought to the deeper groundwater table.

ACKNOWLEDGEMENT

I would like to thank the people without whom I would not have been able to complete this research, without whom I would not have made it through my MSc degree, and without whom I would not enjoy the journey!

My thesis research team at the University of Twente, especially to my first supervisor, Dr. Ir. R. Van Der Velde (Rogier); my first supervisor, whose insight, knowledge and experience into the subject matter always directly guided me through this interesting research. Also, special thanks to Dr. Ir. C. Van Der Tol. (Christiaan), who supported me besides providing academic knowledge and managed to pass the way smoothly.

Also, I would like to thank Prof. Dr. Z. Bob Su, for his time to improve this research.

Thanks to Dr.Ir. T.A. Groen (Thomas) for reading this research and his efforts in the Master of Spatial Engineering (M-SE) program.

My mentor, Arno van Lieshout, supported me and accelerated this research to happen and to be done logically. Thanks Arno!

I want to heartily thanks Drs. T.R. Luiten (Tiny), whom I would never forget how wisely she managed my educational stuff during my MSc. I think the M-SE program should be proud of having her.

My fellow students, Rachel, for her real help and advice, Chiara for her strategies to work hard and enjoy life as well., and Kisanet, a true friend who always motivated me to be brave and positive! We made many memories together; these people are shining in my student life!

Also, I would like to thank other M-SE students who intentionally or unintentionally taught me something!

And my biggest thanks to my family in Iran, my dear Mom, my dear Dad, and my sweet sibling, Negar and Yashar in the US, who all very supportively understood me before coming here to realize my dreams and, through this research, encouraged me to make it happen.

And for my husband Mohsen, my family and best old friend! Thanks for all your warm words and supports; these were like wings that I enjoyed through this journey flying! You are amazing, dear!

TABLE OF CONTENTS

LIST OF FIGURES

LIST OF TABLES

1. INTRODUCTION

This chapter will outline the general background that motivated this thesis to start. It begins with a short motivation, drought concept, and causes that are followed by the problem statement and research gaps. Later, the research questions were defined and subsequently their objectives. In the end, a framework was designed to describe the research objectives conceptually and concisely.

1.1. Motivation

Studies indicate that the Netherlands, during the dry years in 2003 and 2011experianced drought (Van Loon, 2015), where the drinking water demand, river discharge, and navigation affected negatively(UNISDR, 2011). Again in 2018, this country faced a drought but an extreme event that hasn't been experienced since 1976 (Weijers, 2020). Drought is not happening only in the Netherlands; climate change and humans impact the environment on a global scale. Based on the IPCC 2014, there is low confidence in global scale drought trends observation because of less direct measurements, geographical inconsistencies, and dependencies of inferred trends to the definition that is selected for drought (Pachauri et al., 2014). Different continents have different impacts; for instance, the southern part of Europe is becoming drier, while the northern part receives more rainfall (Mishra & Singh, 2010). These fluctuations caused a failure in Spain's 40% agricultural products in 2005. This failure was basically due to the imbalances between demand and supply (Sepulcre-Canto, Horion, Singleton, Carrao, & Vogt, 2012). Besides human life, drought can threaten the natural ecosystem; for instance, 35% of the indigenous plant species in the Netherlands rely on the groundwater, and any management practices or extreme event can affect their ecosystem adversely (NHV, 2004). After the extreme event in 2018 in the Netherlands, a committee of Beleidstafel Droogte by the Minister of Infrastructure and Water Management was established to study drought and represent management recommendations. To make the country more resilient, one task of the committee was introducing a new drought indicator without having limitations of the current. This indicator is precipitation deficit, and one limitation is using reference evaporation as an input (Weijers, 2020) that cannot make the indicator an actual representative. At the same time, free gridded datasets generated from global models are accessible and used for different purposes (Schumacher et al., 2020).

So the sentences above show that drought hazard can affect many ecosystems and consequently many stakeholders. The Netherlands experienced drought in recent years, and the government allocated a budget to quantify it for future policies.

This research aims to investigate global models' applicability and also in-situ measurements as different drought indicators to study it comprehensively. The global models represent actual parameters, not the theoretical. Also, non-climatic causes can be investigated using local in-situ measurements like groundwater tables. To do that, this research continues with elaborating in drought concept and definitions in the following.

1.2. Drought Concept

However, there is no universal definition for drought (Lloyd-Hughes, 2014); some well-known organizations tried to define it as the below (Table 1).

Table 1 General definitions of drought

Organization	Definition
World Meteorological Organization (WMO) https://public.wmo.int/	a slow creeping natural hazard that occurs due to the natural climatic variability
Intergovernmental Panel on Climate Change (IPCC) Report 2019 https://www.ipcc.ch/	A period of abnormally dry weather long enough to cause a serious hydrological imbalance.
Food and Agriculture Organization (FAO) http://www.fao.org/	It is a complex natural phenomenon with varying levels of intensity, duration, spatial extent, and impacts.
Emergency Events Database (EM-DAT) https://www.emdat.be/	A Natural-Climatological hazard caused by long-lived, meso- to macro-scale atmospheric processes ranging from intra-seasonal to multi-decadal climate variability
World Health Organization (WHO) https://www.who.int/	Drought is a prolonged dry period in the natural climate cycle that can occur anywhere in the world.

In another approach, drought is defined conceptually by considering the main stages of progress in a region (Malik, Kumar, & Salih, 2020), which means meteorological, agricultural, hydrological, and socio-economic drought stages (Wilhite & Glantz, 1985). Figure 1 shows the drought propagation conceptually (Van Loon, 2015).

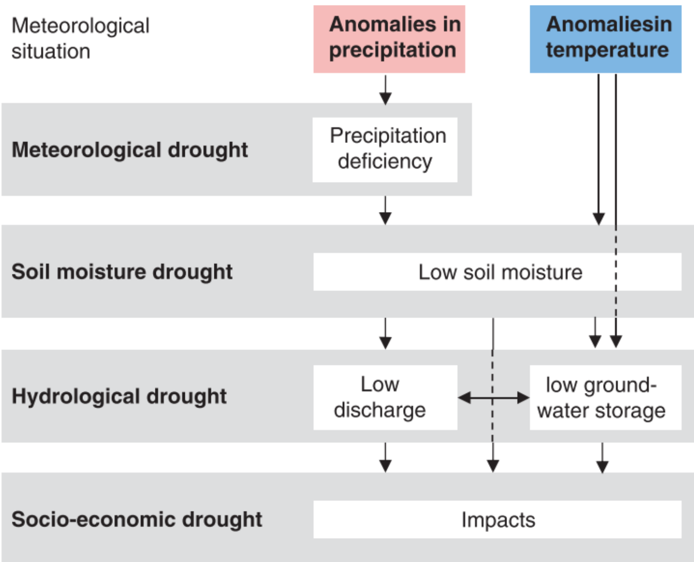

Figure 1 Drought stages (Van Loon, 2015)

- As indicated in Figure 1, anomalies in precipitation trigger meteorological drought, which is defined as less precipitation than the normal amount (Van Loon, 2015). Some references relate the anomalies in temperature to the precipitation deficiencies, which are caused by higher global surface temperatures (West, Quinn, & Horswell, 2019). It is worth saying that this short stage of drought (1 to 3 months deficiency in precipitation) due to the global atmospheric behavior has potential long-lasting and spatial impacts on water availability (Zaniolo, Giuliani, Castelletti, & Pulido-Velazquez, 2018).

- Once meteorological drought occurs, less-than-normal soil moisture is probable that directly affects vegetation coverage and consequently agricultural productivity, which is called agricultural drought (Mishra & Singh, 2011).
- Meteorological deficiencies affect water availability, so water resources, either surface or groundwater, are influenced if drought progresses. The negative influence of these hydrological resources, like streamflow and groundwater resources, is identified as hydrological drought. This stage of drought can persist longer than the meteorological drought (Wilhite & Glantz, 1985).
- Finally, good demand exceeds supplies when society and the human population are affected by the drought stages (West et al., 2019), which is called a socio-economic drought (Mishra & Singh, 2010).

Drought assessment is part of proper water resources management and planning (Malik et al., 2020). There is not a universal definition for this disaster, but it is received that this is a dynamic and slow hazard that lack of universal definition have made it wicked for organizations as defining the relevant affected stakeholders is not easy according to their definitions. The above conceptual definition decreases the wickedness as it looks at this hazard dynamically by defining the stages that each has different characteristics. Therefore, the drought concept in this research is based on the conceptual definition, which represents a comprehensive view of drought and can also be used for administrative purposes who establish policies.

1.3. Drought Causes

Precipitation deficiency is the primary driver for drought hazard occurrence; however, drought can be computed spatial-temporally based on the impact context (Sepulcre-Canto, Horion, Singleton, Carrao, & Vogt, 2012). This section discusses a general background of the reasons for drought occurrence or worsening the impacts. By these items, drought in a region can attribute to the climate or humans.

1.3.1. Climate

Average global Earth's surface temperatures have increased globally over the last 157 years based on IPCC report 2014 (from 1880 to 2012), estimated to be near 0.55 oC since 1970s. Global warming can exacerbate drought hazards, and half of the terrestrial lands that are fertile or suitable for agricultural production on the Earth are susceptible to droughts impacts (Mishra & Singh, 2010). Depending on the regional characteristics, drought impacts can last for some months or years (Balti et al., 2020) on a large area (Nagarajan, 2010). Based on the climate scenarios, the middle part of Europe, where the Netherlands is located, will become drier but is still a less certain region to forecast than other parts of Europe (KNMI, 2019). Since before, there are different programs in the Netherlands to analyze long-term surface or subsurface freshwater resources on a national scale due to climate change like the Dutch Delta Programme (Prinsen, Sperna Weiland, & Ruijgh, 2015). Climate scenarios in KNMI'14 show a shorter drought return period in the future, which means this hazard is more probable to occur (Ibrahim & Usman, 2020). Also, Rhine and Meuse rivers' mean discharge increases, but there is a general drier tendency towards more discharge in spring and less discharge in late summer (Weiland, Bouaziz, & Beersma, 2014).

1.3.2. Anthropogenic Drought Causes

Two-thirds of the Netherlands is under sea level. In 900 to 1300 AD, a warm climate period in Europe caused lands desiccation and groundwater table decline in the Netherlands, together with significant agricultural activities on peatlands. These activities caused land oxidation and irreversible subsidence, leading to a relatively low land that is vulnerable to sea-level rise (Weijers, 2020). There are also extreme events from high rainfall, storm surges, and river flood in the history of the Netherlands year 1916, 1926, 1953,1995, 1998, 2000 that threaten society or cause inconvenience and led to many intervention constructions against flood. These events caused more collaboration among stakeholders from other countries. For instance, water management policies, in the year 1995, after peak discharges on Rhine and Meuse rivers, motivated to build integrated transboundary water management, rehabilitate the water system, improve water quality, and protect indigenous plant life in the basins. Besides, at the national level, in 2001, the Government and Parliament adopted "A Different Approach to Water" that enforces to retain and confirm enough space for rivers that. Though many efforts are made to improve water management and planning, the term drought has not yet been defined in the hydrology dictionary of the Netherlands (Moors, Ellen, Mol, & Swart, 2002). In the Netherlands, water consumptions of drinking water and industry are negligible compared to groundwater flushing and agricultural activities (Haasnoot, Van Deursen, Middelkoop, Van Beek, & Wijermans, 2012). Evidence indicates IJsselmeer and Markermeer lakes, as the main water reservoirs located in the Lower Rhine Delta, cannot supply the entire freshwater demands in the dry periods (Prinsen et al., 2015). So, it can make a long-lasting footprint on the hydrological resources during droughts. For instance, some industrial sectors need high water quality for their products. During drought periods, they can extract more that depending on the drought duration; persisting peak demand will happen while the water supply is the same or low. In this period, the industrial company can increase their groundwater extraction, and a persistent decline will occur on groundwater resources. This stress is applied to the groundwater resources because the regulated policies enforce the supply company to exceed the allowed groundwater extraction amount due to compensation for the peak demand, and this consequently enables the industrial sector to extract more (Weijers, 2020). Therefore, water management practices and policies still need to be examined since these are tools for water allocation or distribution among different sectors and can alleviate drought in a region.

1.4. Problem Statement

As mentioned in the previous sections, the Dutch approach towards integrated water management in the transboundary river basins, Rhine and Meuse, focuses more on flood prevention. It is mainly tried to drain water from lands to remove excess water. However, in the years 2003 and 2011, the Netherlands faced water scarcity problems (Van Loon, 2015)and (Prinsen et al., 2015), which is not comparable with the year 2018, when an extreme event had very different records. The summer of 2018 in the Netherlands is characterized by low precipitation and high temperatures. It caused damages to the property of various stakeholders with an estimated amount of 450-2080 million Euros (Hekman, Läkamp, van der Kooij, van de Velde, & van Hussen, 2019). By qualitatively and quantitively influencing the agriculture, drinking water, industrial and navigation sectors (Haasnoot et al., 2012) besides natural ecosystems like indigenous plant life, which relies on the groundwater resources suffered (NHV, 2004). It happened because demands increase during dry periods, and the main water reservoirs supplies are not sufficient. Some freshwater resources are in danger of salt intrusion, so during drought periods (Prinsen et al., 2015) high amount of water is flushed to maintain adverse impacts of groundwater extraction, as the freshwater resources are at risk of rising sea levels and being salty(Haasnoot et al., 2012). Although drinking and industrial water consumptions are negligible compared to flushing, some only extract high water quality that, consequently, during dry periods, makes these resources more vulnerable (Weijers, 2020).

In the Netherlands, the precipitation deficit is currently used as a drought indicator. It has limitations due to using theoretical assumptions to derive the indicator, which will not accurately estimate the situation. Besides, the theoretical background using only climate variables will not be helpful in catchments where many human interventions increasingly apply to water management. So, drought quantification or further policy regulation doesn't seem to be useful enough to utilize this indicator by itself. On the other hand, different areas in the Netherlands don't suffer similarly. To understand it, the current map visualized by KNMI using 13 stations data of precipitation and reference evaporation is provided in Figure 2.

.

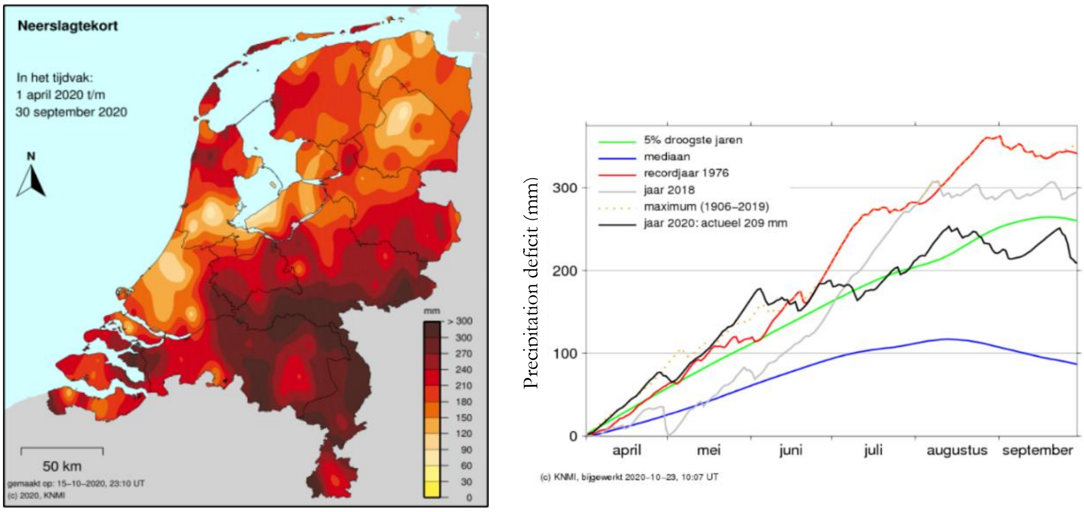

Figure 2 Spatial precipitation deficit in 2020 over the Netherlands b) Temporal precipitation deficit over the Netherlands in dry years and mean conditions.

After the recent years, the damages to various stakeholders indicate current methods no longer respond to future droughts. Based on the reasons above, water management planning in the Netherlands needs to be improved or integrated with drought assessment, especially for vulnerable regions far from main water storages where groundwater is the primary water resource. **So, in one statement, the problem is: in the Netherlands, the drought stage is not yet clear, and the current quantification methods were not efficient in recent drought years.**

1.5. Justification and Research Gap

To analyse drought, some challenges have made it wicked and considered a research gap for the previous studies and are explained one by one in the following.

First, as drought impacts are specific for a region, choosing an appropriate index might be wicked. After an event, many indicators and indices are already being introduced by authorities and stakeholders to explain drought hazard, monitor the impacts, and examine the applicability of current drought policies for future events (Lloyd-Hughes, 2014). World Meteorological Organization (WMO) and Global Water Partnership (GWP) categorized them into four groups of meteorological, hydrological, soil moisture, spectral or remote sensing, and composite based on indices i) ease of use, ii) their input indicators, and iii) the study purpose (WMO handbook 2016). Normalized Difference Vegetation Index (NDVI) is the most frequent spectral indices to monitor agricultural drought or vegetation stress (West et al., 2019); however, this index cannot be representative to estimate vegetation health caused by water stress because it is not clear whether the stress happened by drought or diseases (Sepulcre-Canto et al., 2012). In the Netherlands, the current drought indicator faced some deficiencies that the committee of Beleidstafel Droogte established to introduce an indicator without the previous limitation. This study still sees an opportunity to evaluate this current indicator using actual input data and also in combination with other variables.

Secondly, which dataset to be used is another challenge for drought assessment in a region. Land surface indicators such as precipitation or soil moisture can be derived from Land Surface Models (LSMs) (Spennemann, Rivera, Celeste Saulo, & Penalba, 2015). For instance, Global Land Data Assimilation System (GLDAS), as one of the most widely used models (Rodell et al., 2004), represents variables such as precipitation, evaporation, and soil moisture (Islam & Mamun, 2015). Another global model is ECMWF Reanalysis 5th Generation (ERA5) that presents actual climate variables and can be used in the meteorological analysis. The reanalysis of precipitation products is more reliable data in humid and tropical regions (Kolluru, Kolluru, & Konkathi, 2020). It is important to note that the reliability of the models is not the same in different areas and changes with altitudes, latitude, or climate conditions. For instance, GLDAS model variables are less reliable in the arid region or mountainous areas (Bi, Ma, Zheng, & Zeng, 2016). The model's performance can be evaluated by comparing them with the in-situ measurements in different regions (Liu, Gu, Xie, & Xu, 2020).

Finally, in drought analysis, accessible data and having a good platform to derive datasets or doing the analysis might be wicked. With a cloud-based platform, Google Earth Engine (GEE) accelerates geospatial analysis worldwide (Noi Phan, Kuch, & Lehnert, 2020) in various applications like vegetation monitoring, landcover mapping, and disaster management. The data can be uploaded from the archive that stores massive datasets from different satellites (Mutanga & Kumar, 2019). Different functions are available in the GEE that makes the analysis possible. The interactive and user-friendly environment provided more understanding of the data analysis for the users (Tamiminia et al., 2020). Therefore, to comprehensively assess drought impacts, the cloud-based user-friendly environment of the GEE accelerates the computation and decreases wicked data analysis, especially for beginners users.

So, to overcome drought impacts in the Netherlands, the use of the actual evaporation and global models simulation has not been investigated for regional drought analyses. Moreover, the drought's conceptual definition and comprehensive analysis show drought propagation in every region develop differently. By considering local in-situ measurements and comparing different indicators, someone can interpret drought progress or the stage in one area aimed in this study. In the Netherlands, observational data is freely accessible and has a good density; it is an opportunity to observe the models' capability in a perfect place regarding in-situ measurements.

So in one statement, the solution that will assess in this study is **the integrated use of global models and in-situ measurements to analyze the drought stage in the Netherlands and improve the current quantification methods are the research innovation that approaches drought in the region.**

1.6. Research Objectives and Questions

According to the importance of drought events and the impacts on the groundwater, this research's main objective can be formulated **to assess the drought impact on groundwater in the Netherlands using climate data that derived from long term gridded datasets from GLDAS and ERA5 repositories in Google Earth Engine (GEE)**.

The sub-objectives are defined as follows:

- Derive 20 years precipitation deficit from global model simulations (GLDAS and ERA5) available in GEE on the study area
- Assess the performance of global models simulations (GLDAS and ERA5) compared to the observational data from KNMI in the study area
- Interpret drought impacts in groundwater table from DINOloket in-situ measurements over the datasets overlapped period

So the research questions that will be answered from the above-derived sub-objectives can be formulated as follows:

1. How does precipitation deficit derived from GLDAS and ERA5 change temporally over the Netherlands?
2. How is gridded datasets' performance from models of GLDAS and ERA5 compared to the observational datasets from KNMI over the study area?
3. Is it possible to define a relationship between the precipitation deficit and groundwater table in the study area?

1.7. Conceptual Research Framework

In Figure 3, the datasets, including gridded and in-situ measurements, different processes, and main steps, are shown as a conceptual model for this research. For this study, the Twente region in the Netherlands was selected due to the more vulnerability to drought impacts over the recent years. This is a region in the east of the Netherlands far from coastal areas and lakes storages. So during dry periods, as it has a higher elevation, the sandy slopes faster drain, and groundwater resources are the main high-quality water to be extracted. All these factors motivated this research to choose this region as a study area. It is worth mentioning that the largest grassland in the Twente are the exact areas to study in this research that are explained in more detail in the next chapter.

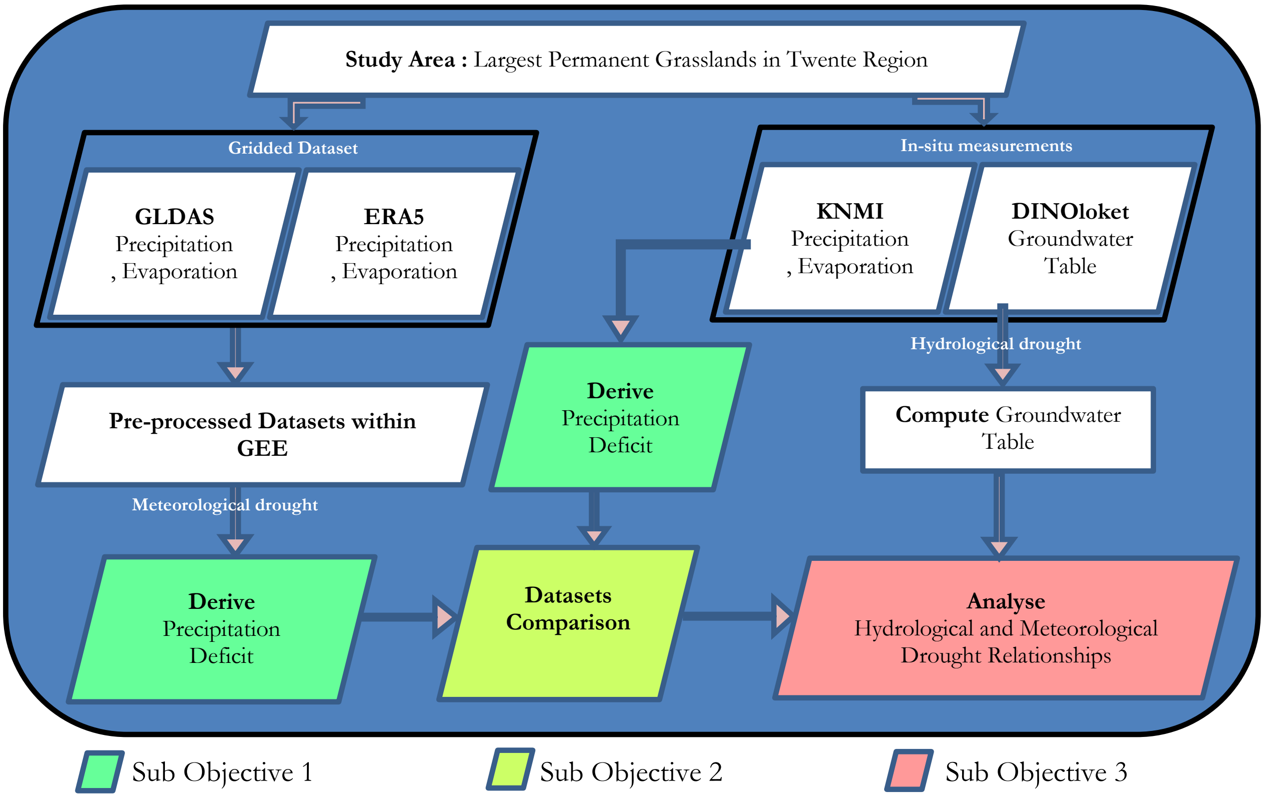

Figure 3 Conceptual Model for the Research

2. STUDY AREA AND DATA

This chapter focuses on the study area and data background of this research. The previous chapter (Introduction) provided details about the problem, research questions, and conceptual model for the entire research. Further information concerning the study area, characterization based on the in-situ measurements, and literature are discussed here.

2.1. The Netherlands' Geography

The Netherlands, with an area of 41543 km^2 has four main river basins of Ems, Rhine, Meuse, and Scheldt (Rijkswaterstaat, 2016). Annual precipitation computed based on six stations De Kooy, De Bilt, Leeuwarden, Eelde, Twenthe, and Eindhoven KNMI station data over 35 years timespan, which varies from 740 mm to 840 mm spatially.

During glacial periods landscape of the Netherlands, particularly the northern half, is strongly influenced. Deep valleys, which present the stream patterns for today, were scoured, and the sandy material pushed into ridges and led to low hills, which are important groundwater recharge areas. These hills are not suitable for agriculture due to a coarse soil material textured and also deep groundwater table. Their cover is mostly planted areas like forests, nature reserves, or recreational areas. Three significant zones are characterized in the Netherlands in terms of their topsoil elevated sandy areas, clayey soils, and peaty soils. The drainage system in the lowlands areas is artificial almost entirely (NHV, 2004).

Also, based on MODIS/Terra+Aqua landcover (V006MCD12Q1) data from NASA Earth Data tool, from Jan 1st, 2019 to Jan 1st, 2020, the main landcovers are water bodies, small cultivated areas, croplands, and urban landcovers with near 90% of the entire area (Figure 4).

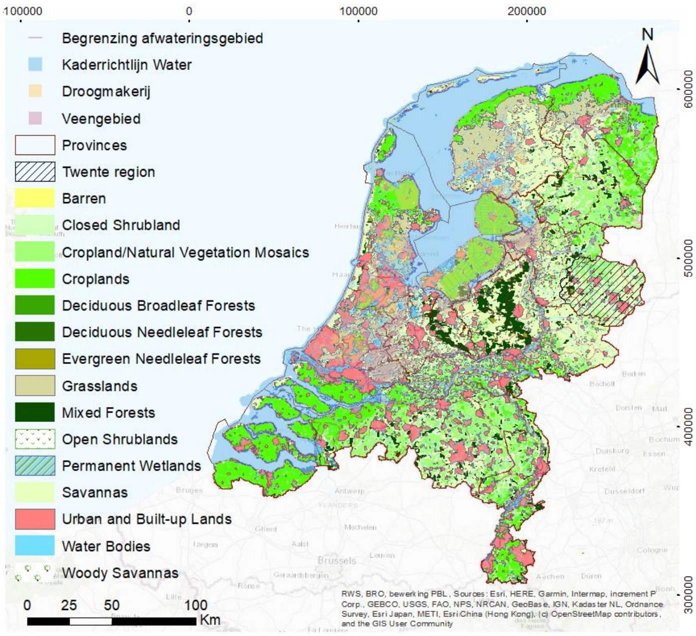

Figure 4 Netherlands landcover derived from product V006MCD12Q1

Croplands and grasslands cover more than 60% of the Netherlands, 13% are built-up areas, and other landcovers near 25%. It is good to mention that the landcover named savannas in Figure 4 is based on the International Geosphere-Biosphere Programme (IGBP) manual, and Woody Savanna or Savanna implies for tree covers 30-60% and tree cover 10-30% (canopy >2m). Besides, it was checked within Google Map by visual interpretation, and these are grasslands with disperse trees.

2.2. The Netherlands' Water Governance

This country is a decentralized unitary state with three main administrative levels for water management that change hierarchically at the national, provincial, and regional levels. Each of these levels has its particular responsibilities (Table 2).

Table 2 The Netherlands Administrative Levels (NHV, 2004)

National Level	
Legislative	Parliament
Executive	Cabinet
Provincial Level	
Legislative	12 Provincial Boards
Executive	Queen's Commissioner and Provincial Executives
Regional and Local Level	
Legislative	37 Regional Water Authorities, 489 Municipal Councils
Executive	Dike-reeve and Aldermen, Mayer and Alderman

This institutional level was built through time; water legitimacy is still an important issue in the Netherlands. In the 20th century, as the participation level increased, many stakeholders like house owners, tenant farmers, and residents asked for flood protection methods and regional management. In 1798 national agency of Rijkswaterstaat was created to administer all water affairs at a national level. In the 19th century, provincial water authorities were established to supervise water boards. Regional Water Authorities consist of water bodies that are part of the main water system, of which Rijkswaterstaat is responsible (NHV, 2004). The water board is authorized at the third in regional level and can reject planning permission by the municipal or even appeal to a higher authority; if the municipality ignores their recommendations of the water board in the Netherlands (NHV, 2004).

Governmental legislative and executive responsibilities are defined in the mentioned three levels highlighted to overcome the socio-economic drought impacts and financial problems. For instance, as mentioned before, the remarkable drought damage to the country in 2018 caused many decisions and budgets to study and prevent further consequences.

2.3. Twente Region

In this region study area is the Twente region, which is part of the Overijssel province and is located in the east of the Netherlands on a border with Germany and an area of 1504 km² (Wikipedia, 2021) (Figure 4). The climate in this region is influenced by the mixture of moist air from the sea and west regions and cold air from lands towards the east. Extreme events of warm and cold weather fairly depend on the wind direction and temperatures well out of -10 to 30-degree centigrade. An example of the extreme is the year 2018 that temperature, evaporation, and precipitation records indicate an exceptional situation (van der Velde et al., 2021). This region is highlighted for the drought hazard as mentioned the main drinking water resource especially in the dry season are groundwater resources, at the same time, this region is far from surface water reservoirs and due to the higher slopes transportation is not possible with the current infrastructures (Weijers, 2020). Furthermore, the soil type in this region is dominantly sand or loamy sand near the surface. Together with the shallow groundwater table, higher elevation, and slopy areas, the region's fresh groundwater resources are vulnerable to drought impacts and water fluctuations (van der Velde et al., 2021). It is worth mentioning that the Netherlands has six 'Regionale Droogteoverleggen (RDO)' boundaries to allocate water during drought periods (Weijers, 2020), and the Twente region is part of RDO Twentekanalen.

So, due to the geographical situation, land surface, and groundwater resources, the Twente region is considered a vulnerable area with priority to study drought impacts. In addition, the boundary is within the provincial Overijssel border and almost within the same water board and RDO boundaries. These same boundaries make consistent administrative legislation and execution at the region that decreases the governance wickedness.

2.4. Observational Data or In-situ Measurements

Climate data from KNMI and groundwater measurements from DINOloket tools are the observational data derived for the Twente region to assess the drought stage and propagation there. The Royal Dutch Meteorological Institute (KNMI) also provides ground-based monthly precipitation amounts from 1974 for different regions and daily precipitations for different stations ('KNMI precipitation,' 2021).

Subsurface data can be viewed and requested freely at the DINOloket application of TNO, the Geological Survey of the Netherlands. It was generated from the DINO database and the BRO or Basisregistratie Ondergrond in Dutch. The groundwater monitoring stations are over the entire Netherlands, and the in-situ measurements are available on the DINOloket platform. More details about the largest Dutch subsurface database and the instruction for using the application are available on the website with the link: https://www.dinoloket.nl/help-ondergrondgegevens ('Ondergrondgegevens | DINOloket,' 2021).

Groundwater wells data are available in the DINOloket database. There are various data available in the BRO data database, such as Soil and soil investigation, Groundwater monitoring and Other research. The dataset includes two data of 'Put met onderzoeksgegevens' and 'Grondwatermonitoringput (BRO)' for groundwater monitoring wells. The BRO provided as txt format and didn't have groundwater tables data but measurements of water quality. The Put met onderzoeksgegevens, however, contains daily or weekly measurements, which is provided in a folder named "Grondwaterstanden_Put." By requesting the data in DINOloket, downloading is possible. First of all, a polygon for a region can be drawn manually from the available tools in the database. Also, it is possible to download data for a defined border, like a province, but if the data amount contains more than 5000 wells, it is required to manage it manually.

For this research, an estimated boundary of the Twente region by the polygon tool in the DINOloket was initially drawn. In the ArcMap environment, the CSV point data opened and intersected with the Twente boundary. The data include groundwater tables in centimeters, and it is represented based on three different references of MP (Meetpunt), MV (Maaiveld), and NAP (Nieuw Amsterdams Peil) which are respectively referred to a measuring point, a surface level, and the new Amsterdam level (DINOloket, 2021).

2.5. Gridded Datasets

In this study, global models of GLDAS and ERA5 represent gridded datasets. The model output of ERA-5 and GLDAS-2.1 on a regional scale can provide detailed information needed to estimate the precipitation deficit.

2.5.1. GLDAS

GLDAS drives multiple offline land surface models. Offline means the model doesn't couple to the atmosphere model. GLDAS integrates huge observational datasets and executes data at high resolutions of 2.5° to 1 km globally (Rui & Beaudoing, 2020). It has been developed to produce reliable, available, high resolution, and near real-time land surface fields. These optimal states and fluxes are valuable information for climate and weather forecast models because terrestrial water and energy stores modulate land and atmosphere fluxes. Some techniques are used in the GLDAS modelling procedure to generate an accurate model results, like land surface states reinitialization technique to alleviate the accumulated errors for integrated states like snow or temperature, or a combination of ground-based or space-based data to constrain the states. In more detail, the physical states and fluxes apply to the model by forcing two boundary conditions. First, different Land Surface Models (LSMs), as shown in Table 3Table 3 GLDAS-2 data characteristics (Rui & Beaudoing, 2020), are forced with the observational meteorological variables like precipitation, temperature, wind, pressure, and radiation from GPCC which is a gridded gauge data analysis product and AGRMET which is an agricultural meteorological model that simulate input variables used in agricultural systems, so the atmospheric biases will be avoided. Second, assimilation techniques help the land surface models' states to be more realistic. The global models evolve to estimate better surface energy and water exchange amounts by improving the physical process understanding (Rodell et al., 2004).

Table 3 GLDAS-2 data characteristics (Rui & Beaudoing, 2020)

Contents	LSMs outputs
format	NetCDF
Latitude and Longitude extends	-60° to 90 ° N and -180 ° to 180 °E
Spatial resolution	0.25 °, 1 °
Temporal resolution	3-hourly and monthly
Temporal coverage	GLDAS-2.1: 1st of January 2000 to Present
Land Surface Models	Noah-3.6, CLSM-F2.5, VIC-4.1.2

Input data in NASA GLDAS-2 with three components of GLDAS-2.0, GLDAS-2.1, and GLDAS-2.2. GLDAS-2.0 is forced completely with Princeton meteorological data. In version 2.1 or GLDAS-2.1, the models are forced with both modelled and observational data from 2000 to present using the conditional boundaries from the GLDAS-2.0 simulation. In this version, no assimilation data is done, which is referred to as "open-loop" simulations (Rui & Beaudoing, 2020). GLDAS-2.0 simulation was forced with climate data and radiation fields of NOAA and Global Data Assimilation System (GDAS), Global Precipitation Climatology Project (GPCP), and AGRicultural METeorological modeling system (AGRMET) (Google earth engine, GLDAS-2.1, 2021). Since GLDAS-2.0 is only available to 2010 in GEE, so GLDAS-2.1 is used for the climate data.

2.5.2. ERA-5

Atmospheric reanalysis began in 1979, and ERA5 reanalysis is the fifth generation of ECMWF reanalysis with records from the 1950s. Compared to the previous generations, this version presents higher spatial and temporal data resolutions. This higher resolution permits analyzing weather systems (Hersbach et al., 2020) like the daily total precipitation with 31 km spatial resolution, which outperforms the ERA-interim (Xu et al., 2019). Also, errors estimation and hourly outputs instead of 3 or 6-hourly analysis have been improved (Hersbach et al., 2019). ERA5, an integral component of an assimilation (land data and ocean wave assimilation) system, can also forecast using the improved analysis (Hersbach et al., 2019). ERA5-Land will cover the same period as ERA5 (from Jan 1950 to near present) now covers from 1980 to the near real-time. This dataset is applicable for land studies and is available in GEE as a reanalysis dataset that provided evolved land variables over several decades at an enhanced resolution compared to ERA5 (ECMWF Confluence 2021). It has been produced by replaying the ECMWF ERA5 climate reanalysis land component. Reanalysis is a statistical procedure that using physics laws applied to the various models in ECMWF and together with observational datasets from worldwide build one global, complete, and consistent dataset (Google earth engine, ERA5-Land, 2021).

2.6. Permanent Grasslands

To identify the study area, landcover data derived from Basisregistratie Gewaspercelen (BRP) or crop parcels precisely indicate croplands' boundaries as GIS sheet files for the entire Netherlands. The boundaries of the agricultural plots are based on Agrarisch Areaal Nederland (AAN) or agricultural area (BRP, 2021).

2.7. Data Management Plan

Based on the justification of the hydro-climate variables, spectral indices, and GEE platform, the data management plan can be summarized as below:

Table 4 Data management plan

<table>
<tr><th>Data Type</th><th>Dataset</th><th>Agency</th><th>Variable (Name)</th><th>Temporal Coverage And Resolution</th><th>Spatial Coverage and Resolution</th><th>Update Frequency</th></tr>
<tr><td rowspan="10">Gridded dataset in GEE</td><td rowspan="3">GLDAS-2.1: Global Land Data Assimilation System</td><td rowspan="3">NASA GES DISC at NASA Goddard Space Flight Centre</td><td>Precipitation (Rainf_f_tavg)</td><td rowspan="2">2000 to Present 3-hourly</td><td rowspan="2">-180.0,-60.0,180.0,90.0 0.25 °</td><td rowspan="2">Monthly</td></tr>
<tr><td>Evapotranspiration (Evap_tavg)</td></tr>
<tr><td colspan="4">https://developers.google.com/earth-engine/datasets/catalog/NASA_GLDAS_V021_NOAH_G025_T3H#image-properties</td></tr>
<tr><td rowspan="3">ERA5-Land hourly - ECMWF climate reanalysis</td><td rowspan="3">Climate Data Store</td><td>Precipitation (total_precipitation)</td><td rowspan="2">1981 to present Hourly</td><td rowspan="2">0.25°</td><td rowspan="2">Daily</td></tr>
<tr><td>Evaporation (total_evaporation)</td></tr>
<tr><td colspan="4">https://developers.google.com/earth-engine/datasets/catalog/ECMWF_ERA5_LAND_HOURLY</td></tr>
<tr><td rowspan="2">MOD13Q1 .006 Terra Vegetation Indices</td><td rowspan="2">NASA LP DAAC at the USGS EROS Center</td><td>NDVI</td><td>2000 to present 16-day</td><td colspan="2">250 m</td></tr>
<tr><td colspan="4">https://developers.google.com/earth-engine/datasets/catalog/MODIS_006_MOD13Q1?hl=en</td></tr>
<tr><td rowspan="2">AHN Netherlands 0.5m DEM, Interpolated</td><td rowspan="2">AHN</td><td>DEM</td><td>data taken in springs from 2007 to 2012.</td><td colspan="2">0.5 m</td></tr>
<tr><td colspan="4">https://developers.google.com/earth-engine/datasets/catalog/AHN_AHN2_05M_INT</td></tr>
<tr><td rowspan="4">In-situ measurements</td><td colspan="2" rowspan="2">DINOloket</td><td>Groundwater Table (Put met onderzoeksgegevens)</td><td colspan="3">1971 to present</td></tr>
<tr><td colspan="4">https://www.dinoloket.nl/ondergrondgegevens</td></tr>
<tr><td colspan="2" rowspan="2">KNMI</td><td>Precipitation (RH) and Potential evaporation (EV24)</td><td colspan="3">1951 to present</td></tr>
<tr><td colspan="4">https://www.knmi.nl/nederland-nu/klimatologie/daggegevens</td></tr>
</table>

More information about the NDVI data is available in page 41.

3. METHODS

To study drought, quantify or only qualitatively assess the hazard, someone might be confused about many indices and indicators defined in different pieces of literature; so this chapter starts with looking at the hydrological cycle and water budget in a small watershed. After a description of the physical process, the entire methodology used to answer research questions is presented in the following.

3.1. Hydrologic Cycle

Water moves in a hydrologic cycle along many complicated pathways and over different time scales. For humans monitoring geographical features of interest like a watershed, a dam or reservoir, or an aquifer, the hydrological cycle can be a challenge. A water budget mentions that inflow and outflow water rates are balanced by water storage change (Healy, Winter, LaBaugh, & Franke, 2007) (Equation 1).

$$\text{Flow}_{in} - \text{Flow}_{out} = \text{Change in Storage} \qquad \text{Equation 1}$$

The water budget equation with making a relationship between the input and outputs of a system shows the water transfer. Then a basic Equation 1 can be rewritten as:

$$P + Q_{in} - Q_{out} = \Delta S / \Delta T \qquad \text{Equation 2}$$

Where the components are P as precipitation (mm), E as the total evaporation from soils, water bodies Q_{in} the water flow in the watershed, Q_{out} as outflow out of the watershed, ΔS is water storage changes either the surface baseflow or the groundwater reservoir storages. Depending on the study purpose the Equation 2 is customized. For instance, precipitation can be a summation of rain, hail, snow, rime, or hoarfrost. Water inflows and outflows could be natural and human-induced surface water or subsurface flow. Evapotranspiration can be separated into evaporation and transpiration from other plant surfaces. Water storage within all three land surface atmosphere compartments of the hydrologic cycle occurs. Further refinement could be written as the bellow equation, which is appropriate for many studies.

$$P + (Q_{swin} + Q_{gwin}) - (ET_{sw} + ET_{gw} + ET_{uz} + RO + Q_{bf} + Q_{gwout}) = \Delta(S_{sw} + S_{snow} + S_{uz} + S_{gw}) / \Delta T \qquad \text{Equation 3}$$

Where sw is surface water, gw is groundwater, uz is unsaturated zone; RO is surface runoff, Q_{gwout} is both groundwater flow out of the site and any extractions by pumping, and Q_{bf} is baseflow (groundwater discharge to streams).

The units of all components are the same in mm, and storage changes as computed in a time period of ΔT is mm/unit of time if the annual water budget computes mm/year.

According to the hydrological situation in a region and the study purpose, water budget components can be defined, removed, or added. For this study, the assumptions are the study area is a small watershed with a shallow groundwater system that the boundaries are well defined and ensure no surface water flows into or out except a stream channel that the discharge amount can be measured readily by the methods. If the boundaries correspond to the groundwater boundaries, there is no subsurface inflow as well. So, in this simplified form of water budget Q_{out} is 0 and Q_{in} is a total of R (surface runoff plus baseflow) or ground-water discharge to streams (Q_{bf}), plus the amounts are extracted by humans ($Q^{GW}{}_{out}$). In the Netherlands, the annual changes of storage are measured, and it is on average 300 mm (250 mm to 350 mm). If ΔS_{sw} , ΔS_{snow} , and ΔS_{uz} consider to be negligible and the only change of storage assume to be on the groundwater, then the above equation can be written as bellow:

to compute storage changes in groundwater evaporation can be estimated by the differences of precipitation and streamflow out of the watershed.

$$P -(E +R +Q^{GW}{}_{out})= (\Delta S_{total} - \Delta S_{gw})/ \Delta T \qquad \text{Equation 4}$$

In Equation 4, total evaporation and precipitation influence climate factors, while R and $Q^{GW}{}_{out}$ are affected by human interventions. $Q^{GW}{}_{out}$ changes by pumping and extractions. The water movement porosity coefficient needs to be considered for the groundwater water table changes as the soil limits.

Typically water budgets are arranged in spreadsheets or tables (Healy et al., 2007)

For sandy areas of the Netherlands, the porosity coefficient is between 0.36 to 0.42, meaning every mm of water table change that is measured needs to be multiplied on average by 0.4. The influences and R by a surface runoff if the baseflow is assumed to be constant. In surface runoff generation, the landcover is the main influential factor that is changed by human urban development, and the natural infiltration and water movement and conveyance changes by changing of landcover. There are theoretical methods that relate the runoff volume to the cover and catchment characteristics out of this thesis concept (Naeimi & Safavi, 2019). In this study, as the landcover of the study area is permanent grasslands, the R is assumed to be constant. These assumptions only provided to build a more comprehensive knowledge background for this research; however, the closure of water budget is out of the scope of this research.

3.2. Google Earth Engine (GEE)

Google Earth Engine (GEE) combines a data catalogue of satellite imagery and geospatial datasets to analyze the datasets and is beneficial for scientists, developers, and researchers. The main section to code is code editor, which is accessible via the link code.earthengine.google.com for writing javaScript codes. Other elements of the GEE environment are illustrated in Figure 5. Description of the processing steps used for this research is provided ('Earth Engine Code Editor | Google Earth Engine | Google Developers').

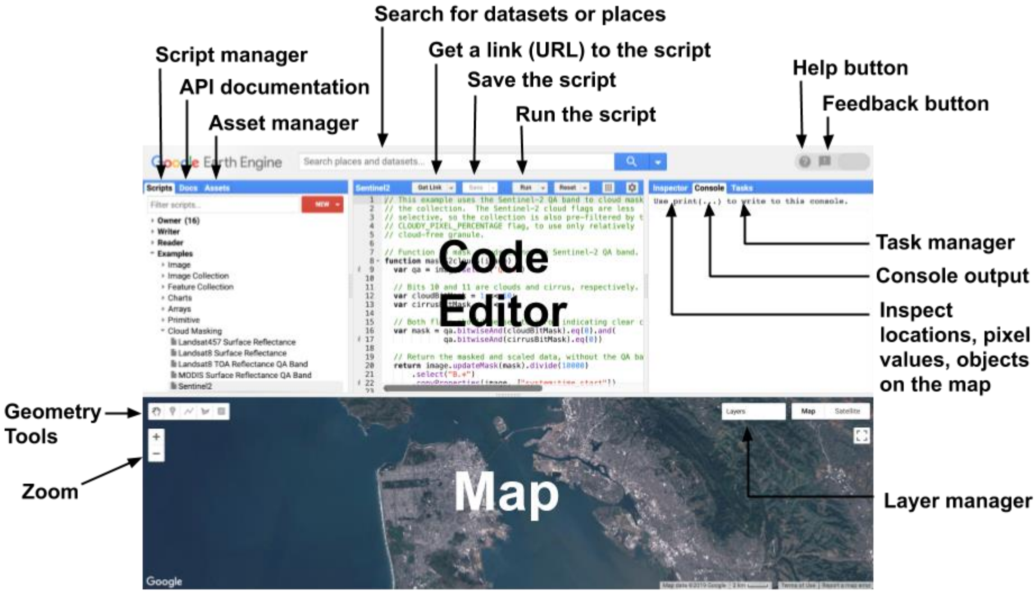

Figure 5 Earth Engine components diagram at code.earthengine.google.com (Earth Engine Code Editor)

3.2.1. Preprocessing

Objects classes in GEE are images, image collection, geometry, features, feature collection, reducer, joint, array, and chart representing the type of data like raster, vector, numbers, or strings.

Each object belongs to a particular class; for instance, an ImageCollection as one object class in GEE includes a stack of images, and each ImageCollection has a specific ID in GEE's data catalog and can be loaded by applying specific function depending on dataset type or ImageCollection constructor. It's good to mention that a complete function list is available in the GEE Docs tab in the JavaScript Code Editor window. For uploading an image collection, it is first necessary to upload the study area in the assets formats shp, zip, dbf, prj, shx, cpg, fix, qix, sbn or shp.xml are acceptable. Then after uploading the dataset, as it is a collection for clipping to the study area needs to do map or shapefile from ee.ImageCollection. To visualize a single day, the day range or to filter for a region, an image collection can be reduced by the commands of .filterDate .filter, or .filterBounds.

3.2.2. Analysis

By taking an input dataset, a reducer produces a single output that is replicated reducer argument automatically to each band by Earth Engine. For example, ee.Reducer.Mean() returns a reducer that is computed using the weighted mean of the inputs and ee.Reducer.First() returns the first of the inputs.

To derive timeseries and download as a CSV excel file, it is better to visualize the dataset because it makes it more understandable. So, after filtering the dataset, using ui.Chart.image.series argument the chart can be visualized in the console tab. ui.Chart.image.series arguments use two inputs, first defining the input image collection and second the border of the study area. The second input reduces the computation to the boundaries, like geometries uploaded to the Asset tab in Figure 5, as a .shp file of the study area. Finally, this function returns a chart.

To download the dataset from task tab of the GEE from (task manager in Figure 5), as it is part of the output process, it will be explained in the next section, but before getting output, it is required to convert an ImageCollection to a FeatureCollection. It is done using the map(function) for mapping the function to all the ImageCollection, .reduceRegion to reduce the computation for the study area, and ee.Feature to convert the prepared ImageCollection to a FeatureCollection.

3.2.3. Output

The output arguments are mainly related to visualization or downloading the data. For visualization, one need is to center or zoom the maps to see the preprocessing or processing. This is done using Map.centerObject(object, zoom) command. The object is the study area and the zoom means a number in this argument from 1 to 24; higher numbers zoom in more at the ends; this command returns a map.

To download or derive timeseries the command written in the code editor to get the time series table can be as a csv file in a desired folder of the google derive the command is Export.table.toDrive which needs to define the input timeseries for that and select the value and date.

3.3. Drought Indicator

(WMO, 2016) defines indices as a representative to represent drought severity numerically using climate indicators. In the following, the drought indicator and an index that is used for this research are described.

3.3.1. Precipitation Deficit (PD)

Precipitation deficit is used by the KNMI as a drought indicator in the Netherlands. So, to make this research consistent with the study area's drought background, this indicator is used for the research. It is defined as total evaporation minus precipitation in a period of time (Equation 5).

$$\mathrm{PD}(\tau) = \int_0^{\tau} E(\tau)\, d\tau - \int_0^{\tau} P(\tau) d\tau \qquad \text{Equation 5}$$

Precipitation and evaporation are both given in millimeters and change during τ, which is the time, and it starts from 1st of April (τ 0). As in the Netherlands, annual precipitation evenly distributes over seasons, but evaporation is highest during summer. This indicator is more applicable during dry months that even more water evaporates in a given period than the amounts precipitated. Due to high temperatures and low precipitation, it is greatest during the summer months. In global models depend on their agreement, E is presented as negative or positive; for this research, the absolute values are considered for E in Equation 5. It is worth mentioning that KNMI uses reference evaporation that is computed theoretically based on a given landcover, climate, and soil condition, which is always more than actual evaporation; for more information, refer to the FAO definition (FAO, 2021). Also, on an average year, water surplus occurs during the winter months and deficit during the summer months.

3.4. Statistical Analysis

To identify anomalies and errors of the datasets or find any relationship by correlation among timeseries, it is required to analyze long-term datasets, which are limited to the period overlapped of different datasets in this research. These statistical analyses and computations are explained in more detail in the following.

3.4.1. Spatio-temporal Standardization and Standardized Anomaly

To compare Spatial-temporal data changes of a variable through time and location, first, it is required to make them comparable. So the standard deviation from long data and for each location is computed as bellow (Gidey, Dikinya, Sebego, Segosebe, & Zenebe, 2018):

$$S_i = \sqrt{\sum_{j=1}^{N_j}(X_{ij} - \overline{X}_i)^2 / N_j} \qquad \text{Equation 6}$$

Where i is the time period, j is the location, N_j is the population or data number, and Si is standard deviation of anomalies at each location of i which is computed for spatial-temporal variables of X in the period of j. $\overline{X}_i$ is the mean that computes for a location as Equation 7:

$$\overline{X}_J = \frac{1}{N_i}\sum_{i=1}^{N_i} X_i \qquad \text{Equation 7}$$

In the end, zij score as a unitless parameter is obtained each observation xij after subtracting the mean of the variable (X_{ij}), and dividing by the value from the last equation, mean anomaly standard deviation, as bellow:

$$Z_{ij} = \frac{X_{ij} - \overline{X}}{S_i} \qquad \text{Equation 8}$$

This Z_{ij} is a standardized anomaly that makes a comparison of absolute variables possible. All of the variables should have the same units and Z_{ij} is a unitless index.

3.4.2. Performance metrics

The performance metrics used in this study include the RMSE, the MAE, and the correlation coefficient (R), which are explained in the following:

- **Root Mean Squared Error (RMSE):**

The models' performances in different studies were evaluated using different methods such as RMSE, which is defined as the below:

$$RMSE = \sqrt{\frac{\sum_i^n (X_{estimation} - X_{measurment})^2}{n}} \qquad \text{Equation 9}$$

$X_{estimation}$ is from the models, and the $X_{measurements}$ is from observations or the reference data that can be considered an actual situation for the model's accuracy. N is the number of data pairs. It needs to put some error bounds on RMSE verification errors. In this study the less RMSE indicates a better stimation for the model, in other words, RMSE closer to 0 (Łabędzki, 2017).
The observational data in this study is considered as KNMI, the reference of the models' variable evaluation.

- **Mean Absolute Error (MAE):**

Another metric is MAE that is computed as below:

$$MAE = \bar{X}_{Predicted} - \bar{Y}_{Observational} \quad \text{Equation 10}$$

$\bar{X}$ and $\bar{Y}$ are the averages of predicted values by the models and observational values from the reference that can be station measurements.

- **Pearson Correlation (R):**

Another metric is R that can compute using $Correl$ command in Microsoft Excel, and it needs some inputs, as explained in the

$$R = Correl\ (X, Y) = \frac{\sum(X-\bar{X})*(Y-\bar{Y})}{\sqrt{\sum(X-\bar{X})^2*\sum(Y-\bar{Y})^2}} \quad \text{Equation 11}$$

Where $\bar{X}$ and $\bar{Y}$and are each timeseries mean value or an array average in Excel.
There is a strong correlation if the coefficient is closer to +1 or -1—the negative correlation between the arrays. A positive correlation means an inverse relationship among timeseries. R equals 0 means there is no correlation. Outliers can cause misleading values and decrease robustness.
This function is also used to identify drought stages relationship. As described in the chapter of the Introduction, drought is a dynamic disaster that progresses in a region, so three different drought stages do not necessarily happen at the same time and might have a lag-time due to the hydrological balance. So, in this research, the timeseries of correlation coefficient with a daily lag is introduced, and the results are provided in the next chapter.

3.5. Groundwater Analysis

All the groundwater wells manually intersected with an estimated Twente boundary in DINOloket and then, after registration on the website, were downloaded via the email address. The visualized map was created for the study area together with all the Twente permanent grasslands provided by pdok in ArcMap (Figure 6).

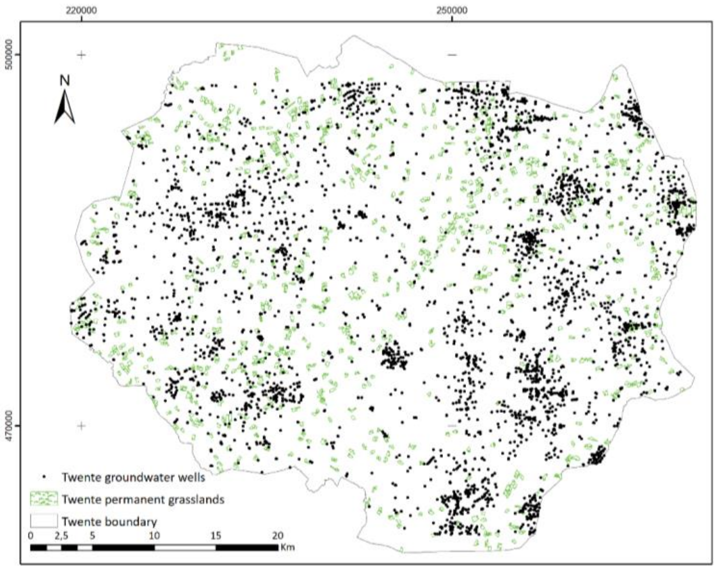

Figure 6 Groundwater wells with research data (Put met onderzoeksgegevens) in the study area

Among lots of fields, the largest fields with an area of at least 6 ha were derived. In some cases, there were two choices: having groundwater well inside the field or closest to the field was given priority. In the Table 5 below, the ten groundwater wells' characteristics that satisfied the criteria are listed.

Table 5 Groundwater wells within ten largest permanent grasslands

NO	ID	Data Availability		X-coordinate	Y-coordinate
1	B34G0251	28/03/1973	22/06/2020	248690	461380
2	B34B0294	29/10/1985	31/12/2019	236362	471788
3	B29C0228	13/09/1985	21/09/2020	264966	477977
4	B29A0158	14/10/1991	31/12/2019	269750	488200
5	B28F0214	15/02/1999	31/12/2019	252567	495878
6	B28D0349	28/09/1979	31/12/2019	235480	483453
7	B28C0180	28/04/1978	31/12/2019	220412	478851
8	B28C0115	07/03/1973	31/12/2019	223423	475932
9	B28B0056	22/02/1971	31/12/2019	231226	494446
10	B28A0063	15/02/1973	31/12/2019	225000	493330

As one part of the results is manually analyzing groundwater tables data in excel, it has been tried to limit the computation by selecting only three of these wells, spreading over the region, as representatives. To do that, from GEE, DEM 0.5 meter of AHN, TIF file derived by coding and the digital elevation model for Twente region visualized in the ArcMap (Figure 7). Then by visual interpretation, three of the wells spreading over the region chose. These are wells located in a different part of the Twente with different elevations, so the geohydrology of these can be different (light blue selected wells in Figure 7 or highlighted box in Table 5).

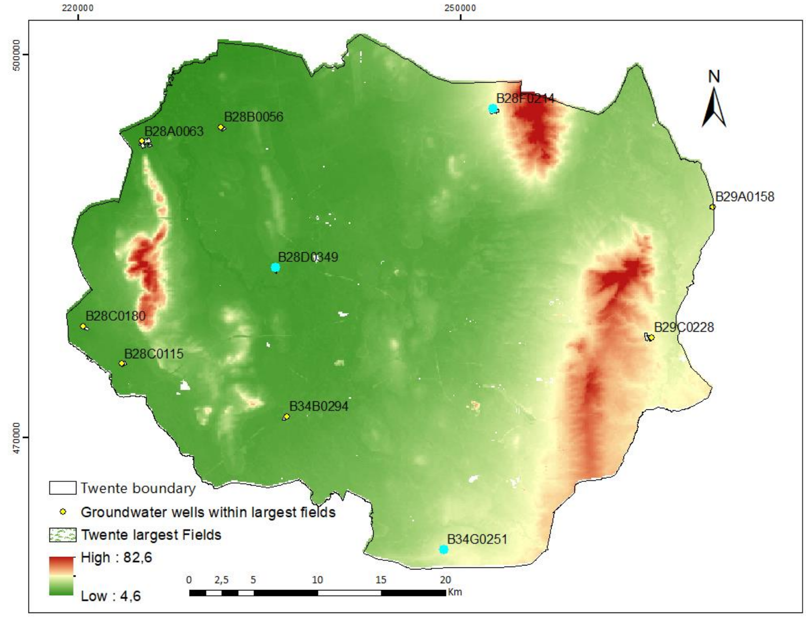

Figure 7 Groundwater wells within larges permanent grasslands in Twente, the Netherlands

Further studies on groundwater tables and fluctuations will be done in the next chapter on the light blue in Figure 7.

4. RESULTS AND DISCUSSION

In this chapter, all the results computed from the mentioned datasets in the second chapter are presented and will be discussed after each result in the same chapter.
The results were derived and analyzed in the GEE, Microsoft Excel, and ArcGIS 10.7.1. The GEE codes are available via the respiratory in https://github.com/GolnarNaeimi/.

4.1. KNMI Precipitation Deficit

For the computation of precipitation deficit (PD) from reference data, the P and ET were downloaded from the KNMI, and after considering outliers az 0 the PD was computed according to Equation 5 for daily values as are shown in Figure 8. Outliers are values less than 0.05 mm written -1 in datasheets that need to be replaced by 0 to refuse influences of -1 into the computations. The potential daily evaporation and precipitation amounts in 0.1 mm are presented in KNM, so these values were converted to mm for the PD. The mean daily values are shown in Figure 8. The driest year is 2018-2019 with a maximum PD of 333 mm and lowes cumulative PD 40 mm (The gray curve ends with +40 mm). As mentioned in the Methods, in the Netherlands, the precipitation is almost evenly divided among different months in a normal year, but evaporation during the summer is higher. However, the year 2018-2019 as the KNMI shows that this year was a very dry year that daily surpluses during winters even couldn't compensate for the entire annual deficit.

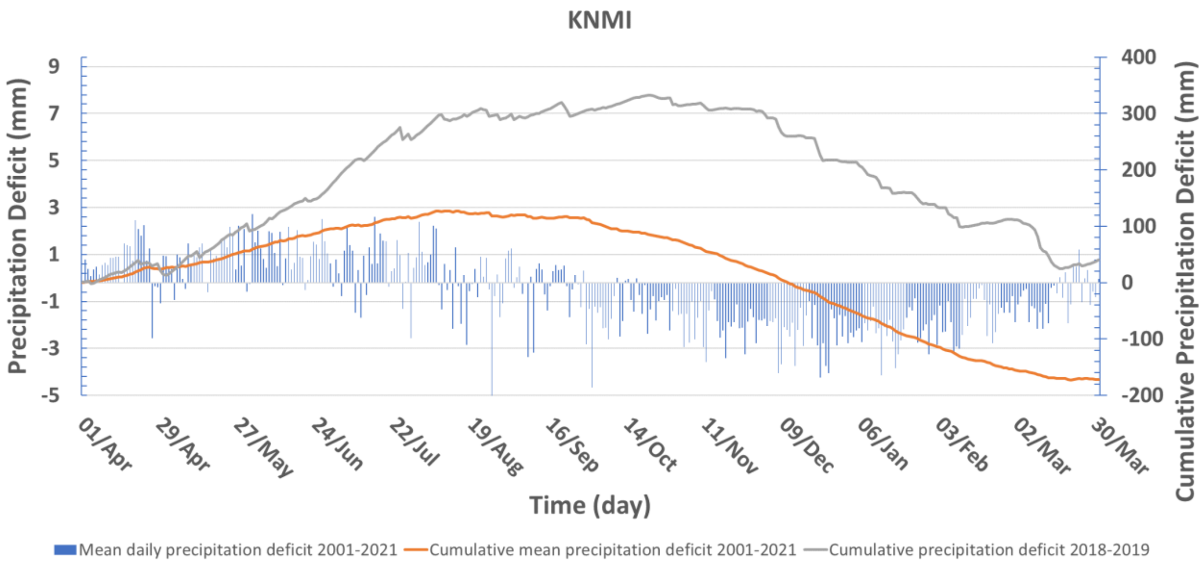

Figure 8 Mean precipitation deficit based on daily data over 20 years data of KNMI (2001-2021)

Figure 8 indicates the maximum and minimum differences in the driest year (in gray), and the mean PD (in orange) almost differentiates are the same September afterward. It also indicates that maximum PD in 2018 occurred more intensively than the normal of the 20 years. It nearly occurred in October. Also, the positive cumulative PD at the end of 2018 shows the evaporation from KNMI during the whole hydrological year was higher than precipitation, but daily values indicate mainly from October. As Equation 5 is used for PD and is about differences in evaporation and precipitation, the positive cumulative PD at the end of 2018 shows that total evaporation by KNMI was higher than total precipitation this year.

4.2. GLDAS Precipitation Deficit

From the GLDAS imagery dataset in GEE's data catalog, 3-hourly data as a CSV file was derived by coding. All the subsequent computation was done in the Microsoft Excel environment. GLDAS data includes precipitation and evapotranspiration as fluxes rates with the unit of kg/m^2/s. So, the first step to compute precipitation deficit was converting the derived rates at each time step to mm/day. As shown with a red circle in Figure 9, the forecast time contains eight time steps of 3-hourly. So, each climate variable's rates are computed in each time step, and then to derive daily values, all the eight computed rates are summed. The computation coefficient that multiplied climate variables at each 3-hours was 3hr*60 min*60 s * 0.5. In fact, a daily value in mm is computed from a summation of 8 areas under the curve based on the eight trapezium areas of 3 hours. In more detail, 0.5 is the average rate for an interval as the rate is not the same for different intervals. Finally, daily precipitation deficits are computed by a summation of all time steps rate values in mm. The explained step has been repeated for all the hydrological years from 2001 to 2021, starting from April to the end of next March. To understand the rates clearly, in a shorter interval and for one day, the beginning and end of a typical forecast time and the general form of the visualized chart in GEE are shown in Figure 9, the values in the vertical axis of this figure as seen are fluxes of GLDAS in kg/m2/s.

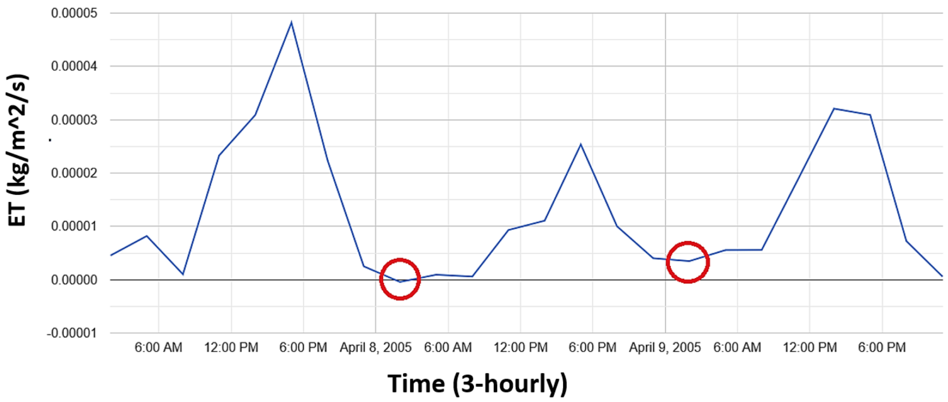

Figure 9 Forecast time in GLDAS and the form of variable rates for a typical ET interval, in GEE console

The computation process repeated to derive annual summations of precipitation deficit to identify the mean and driest year precipitation deficit. The year has the maximum PD of 151 mm and lowes PD of -148mm in the year 2018-2019, the driest hydrological year over these 20 years. So, the mean and driest daily values from GLDAS is shown together in the curve below (Figure 10):

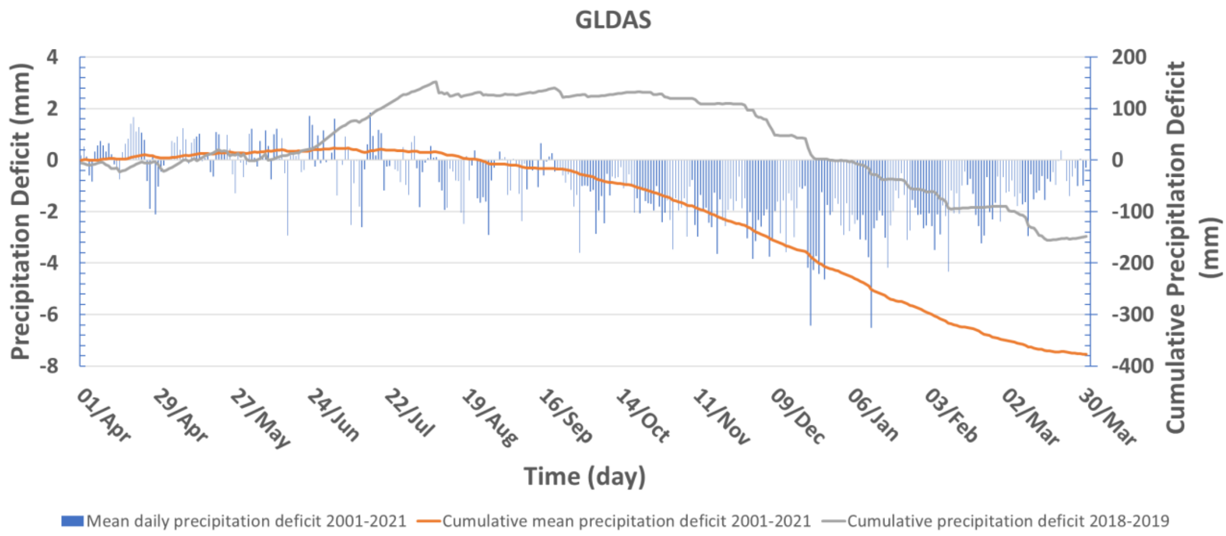

Figure 10 Mean precipitation deficit 3-hourly data over 20 years (2001-2021) derived from GLDAS

To compare two cumulative curves and daily PD inFigure 10, their maximums, differences, and daily values are discussed. Firstly, it is concluded that the high differences between the two cumulative curves started to increase mainly from June. Before that, the PD of the two curves are almost close together. The maximum PD indicates the driest situation, so it is a critical situation from climate. This peak shows the most vulnerable situation. By referring to Figure 8, we can see that the peaks of the curves don't occur simultaneously. Besides the intensive peak, it is showing there was a late summer as the peak in the year 2018-2019 has a shift towards the right. In addition, the driest last 20 years hydrological year based on the PD indicator ends with lower absolute PD compared to the normal situation. It might happen due to the higher potential evaporation than the actual; it is out of this thesis scope, separately looking at precipitation or evaporation. However, from daily values (blue timeseries in Figure 10), GLDAS estimated less evaporation during summer and more precipitation during winter than KNMI. This data station measures rainfall and melted snow; some types of precipitation might have been considered there, so it underestimated the precipitation as it can be other different water types like hail or drizzle. Also, KNMI uses potential evaporation, which has a higher estimation of actual evaporation. The evaporation can be overestimated in KNMI, so these can influence the last cumulative PD amount. In 2018-2019, P from GLDAS by 717.4 mm showed a lower value than normal situation (KNMI: 762 mm and GLDAS: 896mm). Also, the KNMI overestimates the E by 597 mm instead of 569mm.
Figure 10 shows the difference between the two curves is almost the same after October, but their time is not the same. Actually, the curve of dry year vertically stretched and horizontally shifted to the right side, bringing drier late summer that its impacts expand to the winter.

4.3. ERA5 Precipitation Deficit

ERA5 dataset presents hourly data in meters, so there are 24-time steps for each variable. The precipitation and evaporation in this dataset are the total or accumulated amounts in every time step. So, daily values are the last step and the first step differences on a given day.
To understand the general form of accumulated hourly data in ERA5, the hourly data of a typical day within a forecast time is shown in Figure 11below.

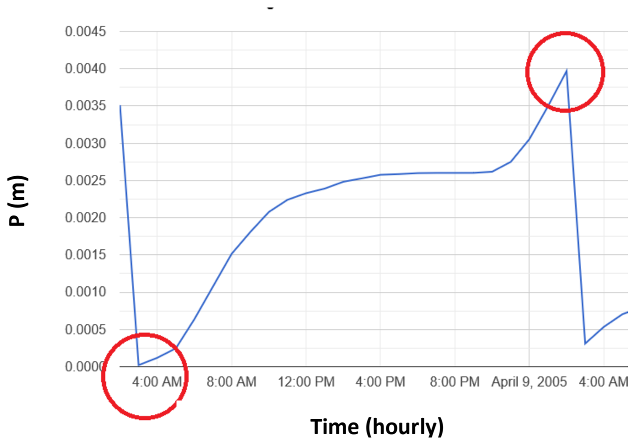

Figure 11 Forecast time in ERA5 and the accumulated variable for a typical interval

The computation process is repeated for all the years, and based on the annual summation of precipitation deficit, the year 2018-2019 has the maximum PD of 191mm on 22 October of 2018 and ends with a value of 56 mm is identified as the driest hydrological year. It has been illustrated with the mean daily values and average comulative PD as the below Figure 12:

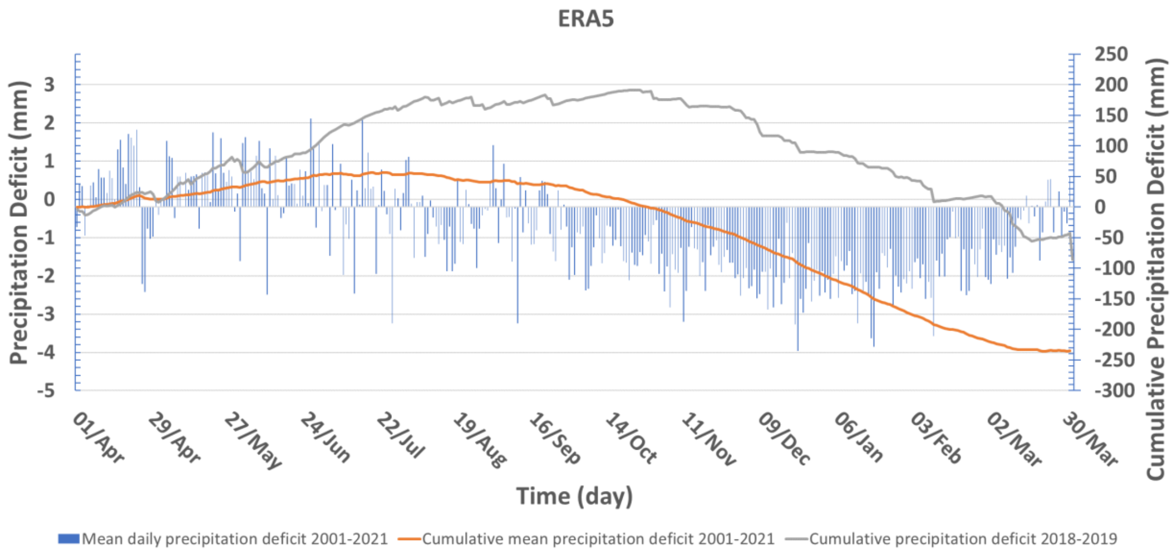

Figure 12 Mean precipitation deficit hourly data over 20 years (2001-2021) derived from ERA5

The differences in ERA5 at the end of the hydrological year are less than GLDAS. Maximum PD, which is a critical situation, is estimating higher in ERA5 than GLDAS.

Interestingly, all three models almost show the same trends and also amount for the normal and dry years differences at the endpoint (around 200 mm).

4.4. Gridded Datasets Comparison

As GLDAS is an offline land surface model and ERA5 is a model coupled with a climate model and some techniques like reanalysis statistical procedures are applied to the ERA5, it seems to be important to check their relationship with in-situ measurements. These datasets, mean annual values for each year computed to show the general differences between the three datasets. For precipitation and evaporation, Figure 13 and Figure 14 show the total mean annual amounts in mm for 20 hydrological years.

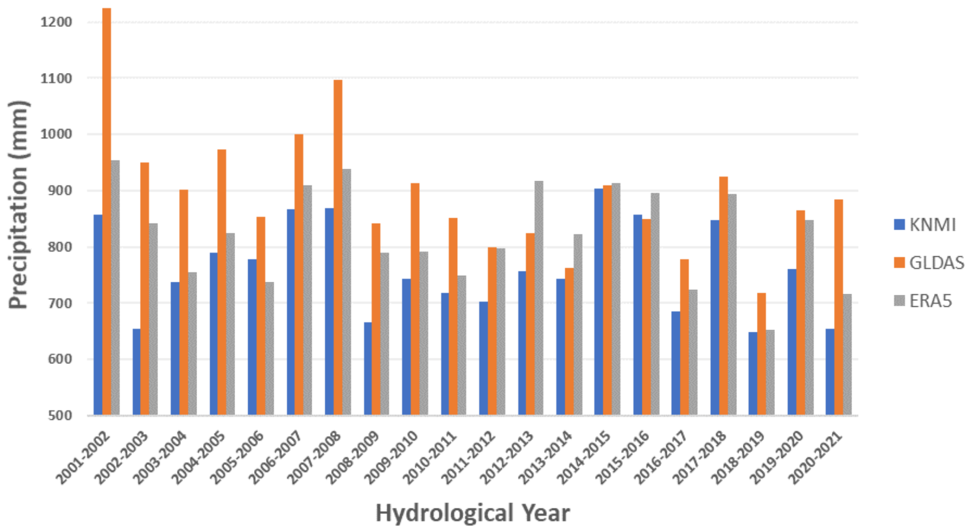

Figure 13 Annual mean precipitation based on average daily data from three datasets over the study area

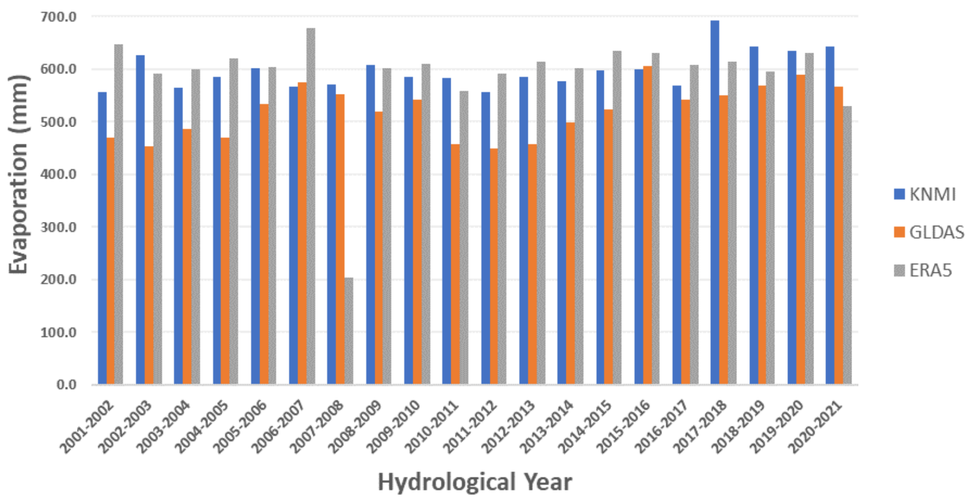

Figure 14 Annual mean evaporation based on average daily data from three datasets over the study area

Then for these values, different RMSE, R, and MAE tests were applied to evaluate the relationship between the model that estimates values and reference data as the KNMI, which is observational values for precipitation and reference data for evaporation. Using Equation 9, Equation 10, and Equation 11, the performance metrics computed and the results of the error tests and correlation between 20 years mean of climate variables from simulated models and KNMI are provided in Figure 15.

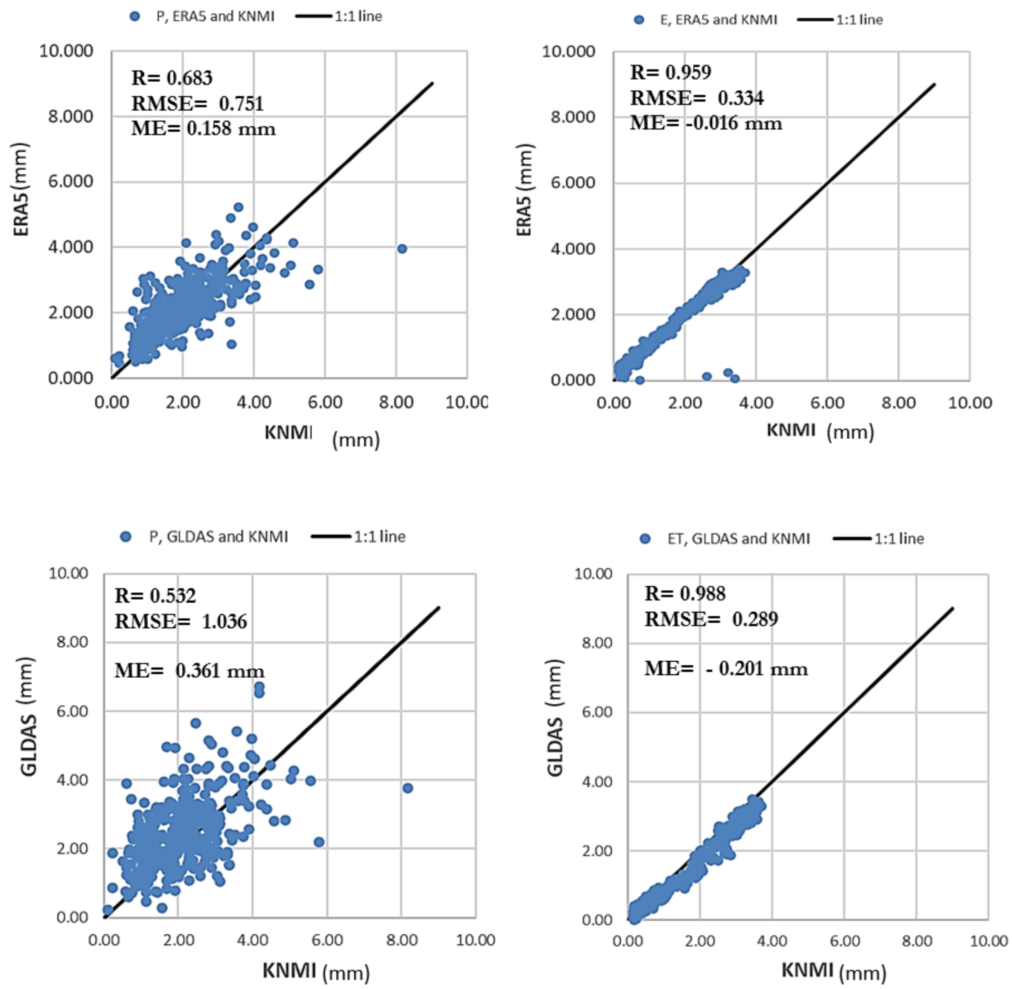

Figure 15 Gridded datasets correlation to the in-situ measurements, P is precipitation, E is Evaporation and ET is Evapotranspiration

The MAE was computed based on the differences of the mean annual of the model variable with the KNMI. The CORREL function in excel is applied to the cell ranges of KNMI and models output to determine the strength of the relationship among two properties.

As mentioned in the Introduction chapter, the gridded datasets can be evaluated using the station data in a region. On the other hand, due to the limitation of station data in PD indicator, which used reference evaporation, it was motivated to use global models to examine their capability. So, the evaporation derived from global models does not correlate with station data, while Figure 15 indicates a very strong relationship between models and KNMI evaporation values. On the other hand, the precipitation data doesn't have that strong relationship with the station data. So, the actual evaporation from the models is very in accordance with the reference evaporation. It might be reliable only for the study area and for other regions can be evaluated since in the Netherlands, as discussed in chapter 2 (Figure 4), near 60% of the area is landcover like croplands, grasslands, and these areas are in accordance with the theoretical assumptions that are used to compute reference evaporation. So, the reference evaporation by KNMI is very correlated with GLDAS and then ERA5 in the Netherlands. But for precipitation, the stronger correlation belongs to ERA5, which estimates total rainfall and frozen water (snow and rain) like the KNMI. GLDAS hasn't been coupled with a climate model, so that might increase the precipitation estimation uncertainty.

Besides the discussion above, some uncertainties need to attention. First, the gridded datasets give one value for a large pixel with different landcovers, not a point or one landcover; for instance, the pixel is here 11.1

km, and comparing that with station data increases the inconsistency and uncertainty. Also, the model's capability to estimate precipitation and evaporation by combining with a climate model and considering boundary conditions in a 3D system for climate variables is increased. As mentioned, ERA5 is coupled with a climate model, so local differences like elevation impacts on the precipitation amount on a regional scale can be improved through the atmospheric estimations. Finally, some other factors like the accuracy of observational data gauge intensity and gauge network coverage affect the uncertainty of working with datasets. As KNMI mentioned in their datasets sheets representing old 70 years old data, the daily time series are not homogeneous due to the station's relocations or changes in observation techniques, which can cause uncertainty.

4.5. Groundwater Analysis

As mentioned in the Methods chapter, three of the wells spreading over the region were chosen (Figure 7). So, in Excel, daily groundwater tables data were organized, and the timeseries were computed. It is good to mention that from 2005 to 2019, only daily values were available (Figure 16).

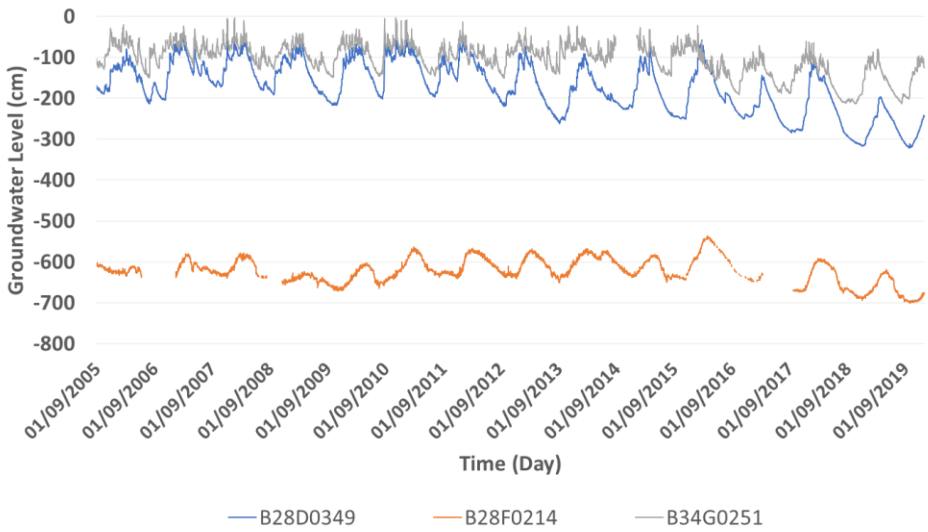

Figure 16 Daily groundwater table from surface

Three wells in Figure 16 indicate different groundwater table fluctuations. The B28F0214, with an elevation of 3100 cm above sea level, has a naturally lower water surface than two other wells. This water table in this well is on average 622 cm below the surface. Two other wells naturally are shallower; the B28D0349 is 172 cm with an elevation of 900 cm above mean sea level, and B34G0251, with an average of 105 cm, is located in a point with 2800 cm height. All the wells' fluctuations indicate a declining trend in groundwater resources of the Twente region.

Figure 16 are absolute values, so standard anomalies are computed instead to make the groundwater table fluctuations comparable across the region. So, the daily groundwater levels below the surface were considered as an input to compute the anomalies (Equation 6 to Equation 8 and presented in Figure 17.

Mean values in black represent an average view for the groundwater table for the period, which shows a persistent drought. The decline is also observable through the decreasing trend in the yearly moving average of their mean presented (the green curve).

As mentioned before, the data after Sept 2005 was only daily, so the computation was limited to after that. Also, the annual moving average considers the 365 days before, so for the first 365 days period, the moving average obviously has not been computed.

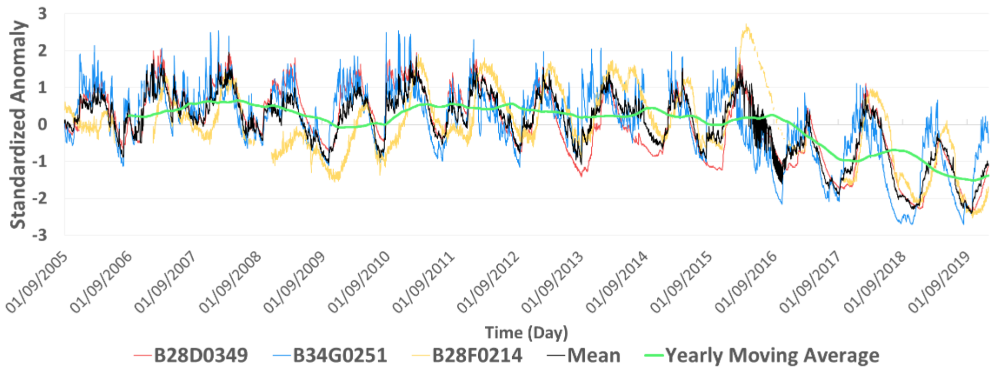

Figure 17 Standardized Anomalies of the Groundwater Wells

Figure 17 shows, the groundwater table in some periods increases like October, and some periods decrease like near April. In general, the trend is a decline in the water table, indicating a persistent hydrological drought in groundwater over the study area. The yearly moving average also marks it, and it is indicated after 2016, there is a faster decline. In recent years, in 2016, there is a turning change in the general trend that anomalies are mostly negative under the baseline or the average, which means the groundwater table in all the wells was below their 14 years. From Figure 17, drought propagation receives differently in the area; for instance, the B34G0251 in the southern part of the study area has faster and more intense drought. As the main soil cover is sandy, this is probably due to the groundwater depth factor in the region in B34G0251 being comparatively shallower. This area is on a high elevation and, consequently, more drainage, making the groundwater resources more vulnerable to drought hazards. So, besides the permanent hydrological drought in the region that indicates the stage of this hazard the southern part of Twente suffering intensively and needs more attention.

4.6. Groundwater Table and Precipitation Deficit Relationships

Two time series of groundwater wells and cumulative precipitation deficits were organized and derived to analyze the Twente region's meteorological and hydrological drought relationships. Regarding a stronger correlation of precipitation derived from ERA5 with KNMI than the GLDAS 2.1 (discussed in section 4.6), the ERA5 was used as a meteorological input for this section.

To select a period to do the analysis, four-time series of groundwater and ERA5 daily means times were overlapped. The period from Sept 2005 to Jan 2020 contains all the meteorological and hydrological daily data. So, over this period, and with an assumption of a linear trend, their linear regression equations were derived for each groundwater measurements (Figure 18). It is good to mention that the precipitation deficit starts from -80.71 cm because the previous main origin was the year 2001. It is good to mention that if these results use for a water budget closure, then the -80.71 value needs to be considered zero for the ease of entering other components on the water budget equation.

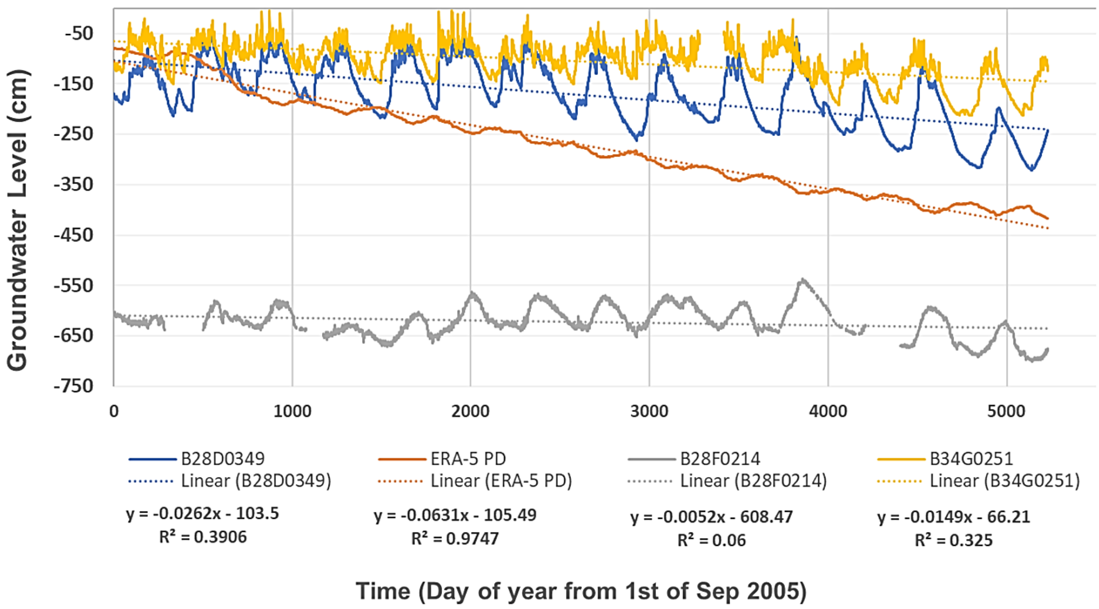

Figure 18 Groundwater table and cumulative daily precipitation deficit

Figure 18 shows a linear equation represented for all the wells and also the PD. Regarding the linear equations in this figure, the groundwater table is naturally deeper in the B28F02014 (the gray timeseries) than other wells.

The next step is detrending or removing the linear trends from these timeseries for easier comparison. So, new values were derived using the linear regression equations, represented in Figure 18, which are named trend values and were decreased from the real groundwater (Figure 19). A negative relationship between precipitation deficit and groundwater tables fluctuation caused to show the secondary axis inversely. For the deeper groundwater table area, the fluctuation to the deficit is not as fast as shallower tables in the well B34G0251. The year 2018-2019 has the max PD of 191 mm on the 22 Oct, which is labeled in the timeseries. Mean water level and elevation in the groundwater wells points are also provided.

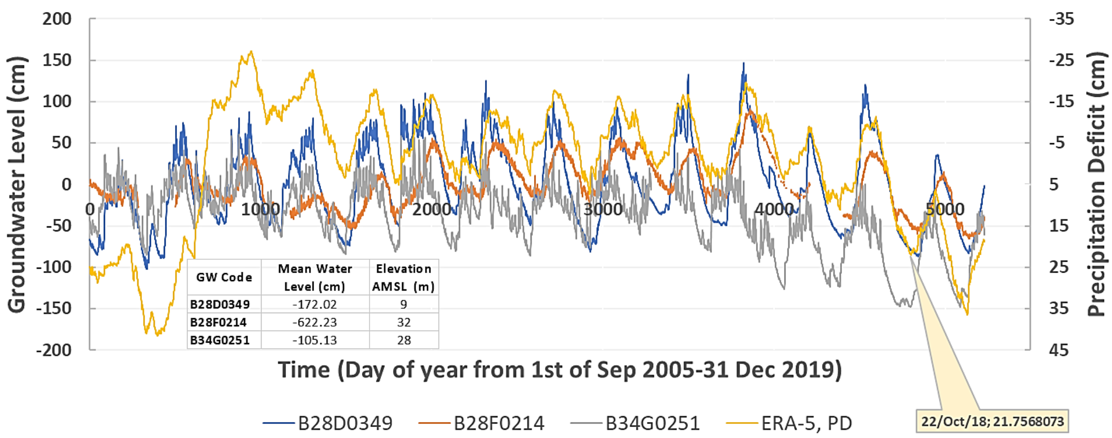

Figure 19 Detrended groundwater table and precipitation deficit

Figure 19 indicates that the well B34G0251 earlier than other wells experience drought. The critical climate situation (max PD) in the year 2018 has been illustrated, and at that moment, almost all the wells were in their lowest amounts. However, the severities started some years before (around three years), first in

B34G0251, then B28D0349, and at the end, B28F0214. In other words, drought impacts started from shallow wells and progressed to the deeper well. The shallowest well experienced drought earlier, so this area needs more attention to prevent drought progress to other deep groundwater tables.

Figure 19, besides the time, shows the drought intensity that in the shallower groundwater, an earlier response accompanies higher negative anomalies intensity; however, in the deeper groundwater, the intensity is lower. It indicates shallower groundwater wells in the Netherlands can experience drought with more severity. Previously based on the PD computation, it is computed that the dries year is 2018-2019; however, in Figure 19, the negative anomalies started some years before, like 2015-2016 to 2017 that intensified in 2018. It reflects that previous groundwater decline did not recharge or the non-climatic triggers like groundwater extractions intensified the groundwater decline before the extreme climatic drought in 2018.

As mentioned, anomalies didn't occur at the same time, which indicates the meteorological and hydrological relationships are not consistent during the time. To illustrate their relationship, the correlation of three detrended wells and the detrend PD timeseries are derived as below in Figure 20a. As drought is the main objective of this research, highest negative correlations are the critical points that are illustrated with arrows in Figure 20b.

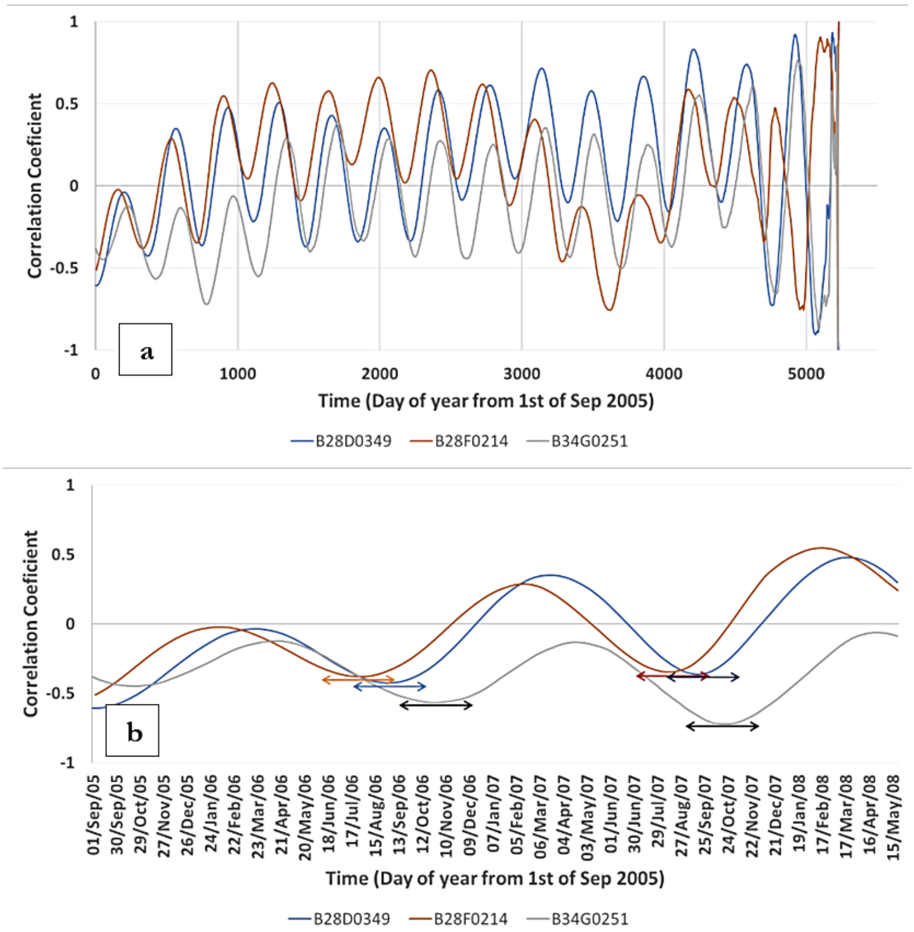

Figure 20 Hydrological and meteorological drought correlation over the complete period b) over the first two hydrological years (line arrows show the highest correlation)

A negative correlation in Figure 20a indicates a negative relationship between the wells table and the precipitation deficits. It demonstrates that when the meteorological deficit is in the highest amount (E>P)

during the summer with the highest evaporation, the groundwater level should be at the lowest level and the same for the period with less evaporation when the groundwater level is in the highest level. Also, spatially, the arrows do not overlap each other. It shows different reactions of groundwater tables to the climate or non-climate changes.
Focusing on two years of hydrological years from April 2006 to April 2008 (Figure 20b), there is a good correlation between PD and groundwater fluctuations (0.5). The highest negative correlations occur when the PD is highest, but it changes through time. The shallowest groundwater well indicates the highest correlation (B34G0251), but with a lag compared to others, it means this well, although was shallower, responds later to PD. It can reflect other non-climate variables that influenced the groundwater table. For this research, water budget closure is not an objective; however, the groundwater decline persistently occurs while there is an annual water surplus or P-E for the Netherlands. The annual amounts computed and a summary are shown in Table 6. This table shows the annual water budget component derived from this study.

Table 6 Water budget components

Data	KNMI	ERA5	B34G0251	B28D0349	B28F0214	B34G0251	B28D0349	B28F0214
Date	**P-E (mm)**	**P-E (mm)**	**ΔG (mm)**	**ΔG (mm)**	**ΔG (mm)**	**ΔSgw (mm of water)**	**ΔSgw (mm of water)**	**ΔSgw (mm of water)**
2001-2002	300	308	-54.4	-95.6	-19.0	-21.8	-38.3	-7.6
2002-2003	27	250	-54.4	-95.6	-19.0	-21.8	-38.3	-7.6
2003-2004	172	154	-54.4	-95.6	-19.0	-21.8	-38.3	-7.6
2004-2005	204	203	-54.4	-95.6	-19.0	-21.8	-38.3	-7.6
2005-2006	177	133	-54.4	-95.6	-19.0	-21.8	-38.3	-7.6
2006-2007	300	232	-54.4	-95.6	-19.0	-21.8	-38.3	-7.6
2007-2008	297	735	-54.4	-95.6	-19.0	-21.8	-38.3	-7.6
2008-2009	57	187	-54.4	-95.6	-19.0	-21.8	-38.3	-7.6
2009-2010	158	180	-54.4	-95.6	-19.0	-21.8	-38.3	-7.6
2010-2011	135	190	-54.4	-95.6	-19.0	-21.8	-38.3	-7.6
2011-2012	146	204	-54.4	-95.6	-19.0	-21.8	-38.3	-7.6
2012-2013	173	916	-54.4	-95.6	-19.0	-21.8	-38.3	-7.6
2013-2014	167	207	-54.4	-95.6	-19.0	-21.8	-38.3	-7.6
2014-2015	307	310	-54.4	-95.6	-19.0	-21.8	-38.3	-7.6
2015-2016	259	260	-54.4	-95.6	-19.0	-21.8	-38.3	-7.6
2016-2017	116	93	-54.4	-95.6	-19.0	-21.8	-38.3	-7.6
2017-2018	156	285	-54.4	-95.6	-19.0	-21.8	-38.3	-7.6
2018-2019	5	38						
2019-2020	125	252						
2020-2021	10	85						
Average	165	261				-21.8	-38.3	-7.6

In Table 6, the water surplus (P-E) based on KNMI is on average 165 mm, and ERA5 and 261 mm. The groundwater table changes are always constant and negative (from each groundwater table fluctuation trend in Figure 1(Figure 18). Also, as mentioned before, to compute water height, the groundwater table changes need to be multiplied by the coefficient of 0.4 to get the net water height. The R and $Q^{GW}out$ are more non-climatic and human influential components that affect the groundwater's natural recharge and extractions. The persistent groundwater decline or hydrological drought roots in non-climate factors in the Netherlands that can be over drainage of water from the lands or groundwater extractions by humans.

5. CONCLUSIONS AND RECOMMENDATION

5.1. Conclusions

The research questions are answered as follows:

RQ1: How precipitation deficit derived from GLDAS and ERA5 is changing temporally over the Netherlands?

For computation of precipitation deficit or PD input data downloaded from the KNMI, GLDAS and ERA5.The in-situ measurements outliers were replaced as 0 and for the models, daily values were computed from in GLDAS, 3hourly data and in ERA5 hourly data. Cumulative mean daily PD over 20 years (2001-2021), mean daily PD, and mean cumulative PD of driest year were computed for all three datasets using GEE codes and datasets. Driest hydrological year for all the three models was 2018-2019, which is illustrated from April to the end of next March. The highest PD is the most critical situation in terms of precipitation deficit, which is for these three datasets KNMI, GLDAS2.1, and ERA5, respectively 333,152, and 191 mm. Also, the end point where the highest absolute cumulative PD was computed and was different for all of them; +40, -148, and -56 mm in KNMI,GLDAS and ERA5. The KNMI curve for the entire 2018-2019 was positive which means very high evaporation and very low precipitation, the water surplus in this year was only 5mm based on the annual KNMI reference evaporation and precipitation differences. By focusing on the year 2018-2019, it seems that there was a late summer as the peak in the year 2018-2019 has a shift towards the right, which occurred later in all the datasets. Interestingly, all three datasets almost show the same for the normal and dry years differences (around 200 mm), but not at the same time or with the same values. The KNMI cumulative PD is always positive and ends positively in March 2019, so this dataset overestimates the evaporation using the reference evaporation compared to others.

RQ2: How is gridded datasets' performance from models of GLDAS and ERA5 compared to the observational datasets from KNMI over the study area?

As discussed in the Introduction chapter, the gridded datasets can be evaluated using the station data in a region. On the other hand, due to the limitation of the current PD indicators in the Netherlands, global models applicability was studied for this research. One part of the evaluation is defined to examine their capability. So, KNMI has been considered reference data, and the metrics of RMSE, R, and MAE are used to evaluate their performance. There is a very strong correlation among models GLDAS2.1, ERA5 actual evaporation, and KNMI reference evaporation values. On the other hand, the precipitation data doesn't have that strong relationship with the station data. It might be due to the more complicated precipitation measurement as water has different phases. So, the actual evaporation from the models is very in accordance with the reference evaporation. It might be reliable only for the study area, for other regions need to be examined, since in the Netherlands, as discussed in chapter 2 (Figure 4), near 60% of the area is landcover like croplands, grasslands, and these areas are in accordance with the theoretical assumptions that are used to compute reference evaporation. So, the reference evaporation by KNMI is very correlated with GLDAS and then ERA5 in the Netherlands. For precipitation, the stronger correlation is ERA5, which estimates total rainfall and frozen water (snow and rain) like the KNMI. GLDAS hasn't been coupled with a climate model, so that might increase the precipitation estimation uncertainty.

Besides the discussion above, some uncertainties need to attention. First, the gridded datasets give one value for a large pixel with different landcovers, not a point or one landcover; for instance, the pixel is here 11.1 km, and comparing that with station data increases the inconsistency and uncertainty. Also, the model's capability to estimate precipitation and evaporation by combining with a climate model and considering boundary conditions in a 3D system for climate variables is increased. As mentioned, ERA5 is coupled with a climate model, so local differences like elevation impacts on the precipitation amount on a regional scale can be improved through the atmospheric estimations. Finally, some other factors like the accuracy of observational data gauge intensity and gauge network coverage affect the uncertainty of working with datasets. As KNMI mentioned in their datasets sheets representing old 70 years old data, the daily time series are not homogeneous due to the station's relocations or changes in observation techniques, which can cause uncertainty.

RQ3: Is it possible to define a relationship between the precipitation deficit and groundwater table in the study area?

To analyze meteorological and hydrological drought relationships, the time series of the groundwater wells from different places in the Twente region and cumulative PD (2001-2021) were analyzed using in-situ measurements data DINOloket.

The ERA-5 model's variables correlated with the meteorological drought indicator from Sept 2005 to the end of Dec 2019, with groundwater fluctuations as a hydrological drought representative. The linear equation of each of the timeseries was derived using linear regression and to observe the anomalies better, standard anomalies were computed when the timeseries detrended (the differences of real values and trend values from linear trend line give a better overview of timeseries to the users). PD and groundwater daily tables fluctuation are inversely strongly correlated. It means when the meteorological deficit is in the highest amount (E>P) during the summer with the highest evaporation; the groundwater level is at the lowest level and the same for the period with less evaporation when the groundwater level is at the highest level. Also, spatially, the correlation peaks (minimums due to the inverse relationships) do not overlap with each other. It shows different reactions of groundwater wells to the PD. The shallowest groundwater well (B34G0251) indicates the highest correlation but responds with a lag than others. It probably happens due to the natural flow of groundwater and the streams that recharge this well. The faster and more intensive reaction of this well to the drought in 2018 started some years before. It happened before the time when the PD was at the highest level, which can prove the shallow groundwater in the southern part of Twente (B34G0251) was affected by non-climatic causes. These can be extractions by humans that exaggerated climate deficiencies, and as the entire Netherlands aquifers are shallow in many parts, drought impacts can spread and influence other areas as well. However, the wells of B28F0214 and B28D0349 are more in accordance with the PD changes, and they have lower anomalies. So, the drought stage in the study area is in the shallow groundwater systems due to climatic and con-climate causes and in deeper groundwater table areas at the stage of climate causes. These impacts can spread to the adjacent areas, so to prevent drought impacts progress; it is recommended to prioritize areas with shallower groundwater table near the well B34G0251. Also, to alleviate drought impacts, it is recommended to investigate artificial recharge methods as the water surplus (P-E) based on KNMI is on average 165 mm or based on ERA5 261 mm.

5.2. Recommendations

In this section, the results and the influential factors that affect uncertainty will be discussed.

5.2.1. Global Models

- As for this study, the landcover was only grasslands, which motivates to consider different landcovers with various behaviors for future works. Figure 21 can give a good understanding of this research study area NDVI, computed using GEE data over 20 years. Regardless of the spatial location, there is consistency among these grasslands; Appendix A for more details.

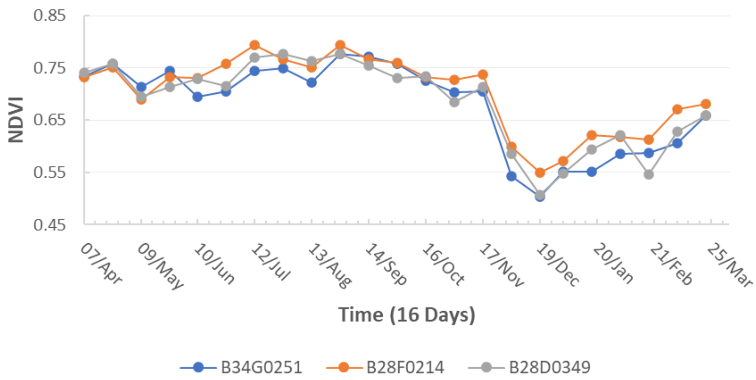

Figure 21 NDVI in three of the largest fields that have a groundwater well inside

5.2.2. Local Patterns

- Datasets perform better globally than on a regional scale that needs to be improved by considering local patterns and influential climatic features (Angélil et al., 2016). Each gridded dataset follows specific input data, algorithms, and specifications that make it prioritized in one region more than others. Also, one dataset depending on the characterization can be more efficient and reliable on one temporal scale. So, choosing different catchments is recommended to evaluate datasets' reliability in other areas as well.
- Moreover, non-climatic factors like human demands in one region or cultural, economic, political background in societies affect water management strategies and decisions. In transboundary catchments where water storage needs to be managed among stakeholders from different countries, a consensus is more wicked, and non-climatic parameters are highlighted—the Twente region part of the Rhine basin recharge from a transboundary river.

5.2.3. Boundaries

- Also, surface water resources boundaries are different from groundwater resources or aquifers. For this study, local wells were analyzed that might increase uncertainty if they are not representative of the same hydrological interaction or have the same water budget components interaction

- It is recommended to integrate future water management scenarios with drought analysis. For instance, the average highest groundwater table or Gemiddelde Hoogste Grondwaterstand - huidig (GHG) provided by Klimaateffectatlas (Figure 22(b)) as a national water model for decreasing damages to agricultural or urban areas due to the high groundwater levels. Figure 22(a) shows average highest groundwater table spatially changes from 0.2 m from the surface to more than 2 meters.

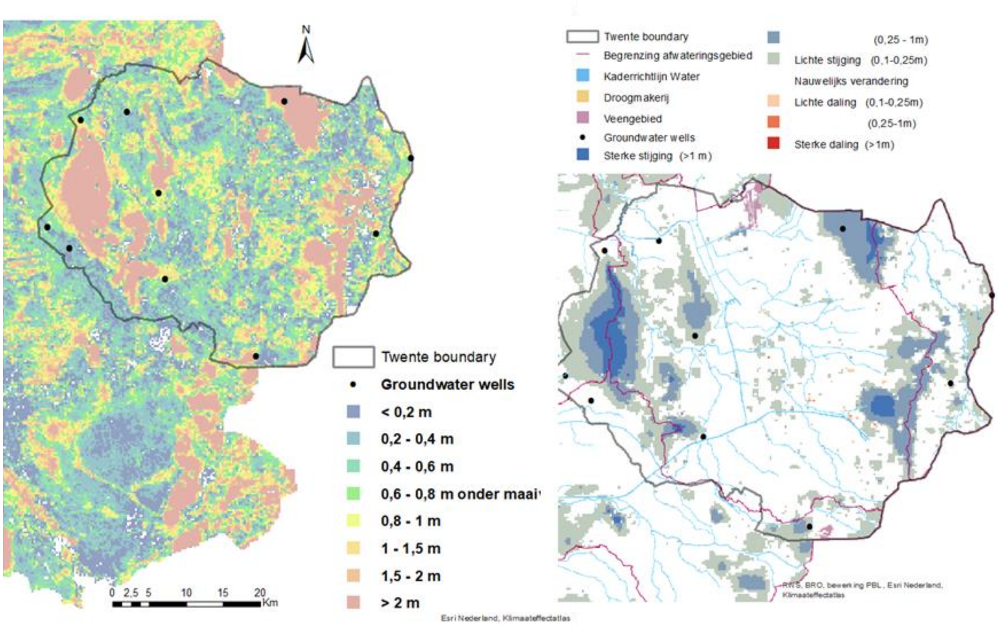

Figure 22 Average highest groundwater table from the surface (left) Average Highest Groundwater Level - 2050 High (right)

- Another recommendation for future works is to identify water boundaries based on the hydrological patterns in the study area. The administrative boundaries for the water allocation are an important border in drought analysis. For instance, RDO responsible for water allocation have an essential responsibility. However, the RDO boundaries seem to include the surface water movements in the Netherlands that need to integrate groundwater areas. It is recommended due to the high tendency of groundwater extraction, especially in areas far from lake storage like the Twente region. In this research, groundwater wells were all in the Twente boundary, but one (B34G0251) was in the southern part of the region with different water allocation regions or RDO that might increase wickedness in applying administrative decisions or water allocations.
- The industrial sector can extract more groundwater during peak demands, such as drought periods when groundwater resources are more vulnerable. It is a gap in their policy and water supply company agreements that need to be modified.

5.2.4. Artificial Recharge

- As the water budget components in Table 6 show, there is an annual water surplus, but there is persistent groundwater decline according to the results of this thesis. Therefore, the extra water can recharge the groundwater artificially using management practices and plans, especially in some vulnerable areas like where the well is located B34G0251. It is required to define the hydrological boundaries initially.

LIST OF REFERENCES

Aksoy, S., Gorucu, O., & Sertel, E. (2019). Drought Monitoring using MODIS derived indices and Google Earth Engine Platform. In *2019 8th International Conference on Agro-Geoinformatics (Agro-Geoinformatics)* (pp. 1–6). IEEE.

Angélil, O., Perkins-Kirkpatrick, S., Alexander, L. V., Stone, D., Donat, M. G., Wehner, M., … Christidis, N. (2016). Comparing regional precipitation and temperature extremes in climate model and reanalysis products. *Weather and Climate Extremes*, 13, 35–43. Retrieved from https://doi.org/10.1016/j.wace.2016.07.001

Balti, H., Ben Abbes, A., Mellouli, N., Farah, I. R., Sang, Y., & Lamolle, M. (2020). A review of drought monitoring with big data: Issues, methods, challenges and research directions. *Ecological Informatics*, 60, 101136. Retrieved 11 September 2020 from https://doi.org/10.1016/j.ecoinf.2020.101136

Bi, H., Ma, J., Zheng, W., & Zeng, J. (2016). Comparison of soil moisture in GLDAS model simulations and in situ observations over the Tibetan Plateau. *Journal of Geophysical Research: Atmospheres*, 121(6), 2658–2678.

BRP (2021). Introductie - PDOK. Retrieved 6 August 2021, from https://www.pdok.nl/introductie/-/article/basisregistratie-gewaspercelen-brp-

FAO. (2021) Chapter 1 - Introduction to evapotranspiration. Retrieved 25 August 2021, from http://www.fao.org/3/x0490e/x0490e04.htm

DINOloket. (2021). Ondergrondgegevens. Retrieved 26 July 2021, from https://www.dinoloket.nl/help-ondergrondgegevens

Dutta, D., Kundu, A., Patel, N. R., Saha, S. K., & Siddiqui, A. R. (2015). Assessment of agricultural drought in Rajasthan (India) using remote sensing derived Vegetation Condition Index (VCI) and Standardized Precipitation Index (SPI). *Egyptian Journal of Remote Sensing and Space Science*, 18(1), 53–63. Retrieved from https://doi.org/10.1016/j.ejrs.2015.03.006

Google Earth Engine, *Google Developers.* (2021). Retrieved 8 August 2021, from https://developers.google.com/earth-engine/guides/playground

ERA5-Land: data documentation - Copernicus Knowledge Base - ECMWF Confluence Wiki. (2021.). Retrieved 18 August 2021, from https://confluence.ecmwf.int/display/CKB/ERA5-Land%3A+data+documentation#ERA5Land:datadocumentation-Introduction

Gallo, K., Ji, L., Reed, B., Dwyer, J., & Eidenshink, J. (2004). Comparison of MODIS and AVHRR 16-day normalized difference vegetation index composite data. *Geophysical Research Letters*, 31(7), n/a-n/a. Retrieved 28 February 2021 from https://doi.org/10.1029/2003GL019385

Gidey, E., Dikinya, O., Sebego, R., Segosebe, E., & Zenebe, A. (2018). Modeling the Spatio-Temporal Meteorological Drought Characteristics Using the Standardized Precipitation Index (SPI) in Raya and Its Environs, Northern Ethiopia. *Earth Systems and Environment 2018 2:2*, 2(2), 281–292. Retrieved 18 August 2021 from https://doi.org/10.1007/S41748-018-0057-7

Google earth engine. (2021). ERA5-Land hourly - ECMWF climate reanalysis. Retrieved 7 August 2021, from https://developers.google.com/earth-engine/datasets/catalog/ECMWF_ERA5_LAND_HOURLY

Google earth engine. (2021). GLDAS-2.1: Global Land Data Assimilation System. Retrieved 7 August 2021, from https://developers.google.com/earth-engine/datasets/catalog/NASA_GLDAS_V021_NOAH_G025_T3H#description

Haasnoot, M., Van Deursen, W. P. A., Middelkoop, H., Van Beek, E., & Wijermans, N. (2012). An Integrated Assessment MetaModel for developing adaptation pathways for sustainable water management in the lower Rhine Delta. *IEMSs 2012 - Managing Resources of a Limited Planet: Proceedings of the 6th Biennial Meeting of the International Environmental Modelling and Software Society*, 1743–1751.

Healy, R. W., Winter, T. C., LaBaugh, J. W., & Franke, O. L. (2007). Water budgets: Foundations for effective water- resources and environmental management: U.S. Geological Survey Circular 1308, 90 p. *Ars Combinatoria*, 95, 65–70.

Hekman, A., Läkamp, R., van der Kooij, S., van de Velde, I., & van Hussen, K. (2019). Economische schade door droogte in 2018 | Rapport | Rijksoverheid.nl, 28–31. Retrieved from https://www.rijksoverheid.nl/documenten/rapporten/2019/12/18/bijlage-1-rapport-economische-schade-door-droogte-in-2018

Hersbach, H., Bell, B., Berrisford, P., Horányi, A., Sabater, J. M., Nicolas, J., … Dee, D. (2019). Global reanalysis: goodbye ERA-Interim, hello ERA5 | ECMWF. Retrieved 10 March 2021, from

https://www.ecmwf.int/en/newsletter/159/meteorology/global-reanalysis-goodbye-era-interim-hello-era5
Ibrahim, I., & Usman, M. T. (2020). Regional differentiation in climate change induced drought trends in the Netherlands Environmental Research Letters Regional differentiation in climate change induced drought trends in the Netherlands.
Islam, M. M., & Mamun, M. M. I. (2015). Variations of NDVI and its association with rainfall and evapotranspiration over Bangladesh. *Rajshahi University Journal of Science and Engineering*, 43, 21–28.
KNMI. (2019). KNMI - Klimaat van Nederland. Retrieved 8 March 2021, from https://www.knmi.nl/klimaat
KNMI precipitation. (2021). Retrieved from https://www.knmi.nl/nederland-nu/klimatologie
Kogan, F. N. (1995). Droughts of the late 1980s in the United States as derived from NOAA polar-orbiting satellite data. *Bulletin - American Meteorological Society*, 76(5), 655–668. Retrieved from https://doi.org/10.1175/1520-0477(1995)076<0655:DOTLIT>2.0.CO;2
Kolluru, V., Kolluru, S., & Konkathi, P. (2020). Evaluation and integration of reanalysis rainfall products under contrasting climatic conditions in India. *Atmospheric Research*, 246, 105121. Retrieved from https://doi.org/10.1016/j.atmosres.2020.105121
Kumar, L., & Mutanga, O. (2018). Google Earth Engine Applications Since Inception: Usage, Trends, and Potential. *Remote Sensing*, 10(10), 1509. Retrieved 17 February 2021 from https://doi.org/10.3390/rs10101509
Łabędzki, L. (2017). Categorical Forecast of Precipitation Anomaly Using the Standardized Precipitation Index SPI. *Water*, 9(1), 8. Retrieved 18 February 2021 from https://doi.org/10.3390/w9010008
Liu, L., Gu, H., Xie, J., & Xu, Y. (2020). How well do the ERA-Interim, ERA-5, GLDAS-2.1 and NCEP-R2 reanalysis datasets represent daily air temperature over the Tibetan Plateau? Retrieved from https://doi.org/10.1002/joc.6867
Lloyd-Hughes, B. (2014). The impracticality of a universal drought definition. *Theoretical and Applied Climatology*, 117(3–4), 607–611. Retrieved from https://doi.org/10.1007/s00704-013-1025-7
Malik, A., Kumar, A., & Salih, S. (2020). *Intelligent Data Analytics for Decision-Support Systems in Hazard Mitigation Theory and Practice of Hazard Mitigation*.
McFeeters, S. K. (1996). The use of the Normalized Difference Water Index (NDWI) in the delineation of open water features. *International Journal of Remote Sensing*, 17(7), 1425–1432. Retrieved 17 February 2021 from https://doi.org/10.1080/01431169608948714
Mishra, A. K., & Singh, V. P. (2010). A review of drought concepts. *Journal of Hydrology*. Elsevier. Retrieved from https://doi.org/10.1016/j.jhydrol.2010.07.012
Mishra, A. K., & Singh, V. P. (2011). Drought modeling–A review. *Journal of Hydrology*, 403(1–2), 157–175.
Moors, E., Ellen, W. van, Mol, J., & Swart, B. (2002). *Hydrologische woordenlijst*.
Mutanga, O., & Kumar, L. (2019). Google Earth Engine Applications. *Remote Sensing*, 11(5), 591. Retrieved 17 February 2021 from https://doi.org/10.3390/rs11050591
Naeimi, G., & Safavi, H. R. (2019). Integrated Stormwater and Groundwater Management in Urban Areas, a Case Study. *International Journal of Civil Engineering*, 17(8), 1281–1294. Retrieved 1 July 2020 from https://doi.org/10.1007/s40999-018-0386-9
Nagarajan, R. (2010). *Drought assessment. Drought Assessment*. Springer Netherlands. Retrieved from https://doi.org/10.1007/978-90-481-2500-5
NHV (2004)-specials - *Nederlandse Hydrologische Vereniging*. (2004). Retrieved 2 August 2021, from https://www.nhv.nu/nieuws/nhv-specials/
Noi Phan, T., Kuch, V., & Lehnert, L. W. (2020). Land cover classification using google earth engine and random forest classifier-the role of image composition. *Remote Sensing*, 12(15), 2411. Retrieved 30 December 2020 from https://doi.org/10.3390/RS12152411
Ogilvie, A., Belaud, G., Delenne, C., Bailly, J. S., Bader, J. C., Oleksiak, A., … Martin, D. (2015). Decadal monitoring of the Niger Inner Delta flood dynamics using MODIS optical data. *Journal of Hydrology*, 523, 368–383. Retrieved from https://doi.org/10.1016/j.jhydrol.2015.01.036
Pachauri, R. K., Allen, M. R., Barros, V. R., Broome, J., Cramer, W., Christ, R., … Dasgupta, P. (2014). *Climate change 2014: synthesis report. Contribution of Working Groups I, II and III to the fifth assessment report of the Intergovernmental Panel on Climate Change*. Ipcc.
Prinsen, G., Sperna Weiland, F., & Ruijgh, E. (2015). The Delta Model for Fresh Water Policy Analysis in the Netherlands. *Water Resources Management*, 29(2), 645–661. Retrieved from https://doi.org/10.1007/s11269-014-0880-z
Rijkswaterstaat. (2016). *River basin management plans 2016-2021 of the Netherlands - Summary*. Retrieved from

https://www.helpdeskwater.nl/onderwerpen/wetgeving-beleid/kaderrichtlijn-water/@178616/samenvatting-sgbp/

Rodell, M., Houser, P. R., Jambor, U., Gottschalck, J., Mitchell, K., Meng, C. J., … Toll, D. (2004). The Global Land Data Assimilation System. *Bulletin of the American Meteorological Society*, 85(3), 381–394. Retrieved 23 February 2021 from https://doi.org/10.1175/BAMS-85-3-381

Rui, H. L., & Beaudoing, H. (2020). README Document for NASA GLDAS Version 2 Data Products. *Goddard Earth Sciences Data and Information Services Center (GES DISC)*, 16(1), 1–32. Retrieved from https://hydro1.gesdisc.eosdis.nasa.gov/data/GLDAS/README_GLDAS2.pdf

Schumacher, V., Justino, F., Fernández, A., Meseguer-Ruiz, O., Sarricolea, P., Comin, A., … Althoff, D. (2020). Comparison between observations and gridded data sets over complex terrain in the Chilean Andes: Precipitation and temperature. *International Journal of Climatology*, 40(12), 5266–5288. Retrieved 10 May 2021 from https://doi.org/10.1002/joc.6518

Sepulcre-Canto, G., Horion, S., Singleton, A., Carrao, H., & Vogt, J. (2012a). Development of a Combined Drought Indicator to detect agricultural drought in Europe. *Natural Hazards and Earth System Science*. Retrieved from https://doi.org/10.5194/nhess-12-3519-2012

Sepulcre-Canto, G., Horion, S., Singleton, A., Carrao, H., & Vogt, J. (2012b). Development of a Combined Drought Indicator to detect agricultural drought in Europe. *Natural Hazards and Earth System Sciences*, 12(11), 3519.

Spennemann, P. C., Rivera, J. A., Celeste Saulo, A., & Penalba, O. C. (2015). A comparison of GLDAS soil moisture anomalies against standardized precipitation index and multisatellite estimations over South America. *Journal of Hydrometeorology*, 16(1), 158–171. Retrieved from https://doi.org/10.1175/JHM-D-13-0190.1

Tamiminia, H., Salehi, B., Mahdianpari, M., Quackenbush, L., Adeli, S., & Brisco, B. (2020, June 1). Google Earth Engine for geo-big data applications: A meta-analysis and systematic review. *ISPRS Journal of Photogrammetry and Remote Sensing*. Elsevier B.V. Retrieved from https://doi.org/10.1016/j.isprsjprs.2020.04.001

Twente - Wikipedia. (2021.). Retrieved 6 August 2021, from https://en.wikipedia.org/wiki/Twente

UNISDR, E. U. R. (2011). Climate change adaptation and disaster risk reduction in Europe: a review of risk governance. *UNISDR and the Council of Europe*.

van der Velde, R., Colliander, A., Pezij, M., Benninga, H.-J. F., Bindlish, R., Chan, S. K., … Su, Z. (2021). Validation of SMAP L2 passive-only soil moisture products using upscaled in situ measurements collected in Twente, the Netherlands. *Hydrology and Earth System Sciences*, 25(1), 473–495. Retrieved from https://doi.org/10.5194/hess-25-473-2021

Van Loon, A. F. (2015). Hydrological drought explained. *Wiley Interdisciplinary Reviews: Water*, 2(4), 359–392. Retrieved 3 November 2020 from https://doi.org/10.1002/wat2.1085

Weijers, R. (2020). Drought indicators in The Netherlands: a case study to support anticipative drought management.

Weiland, F. S., Bouaziz, L., & Beersma, J. (2014). *Comparison of CMIP5 climate model projections and preliminary KNMI'14 scenarios with earlier climate assessments for the Rhine and Meuse*. *Thesis*.

West, H., Quinn, N., & Horswell, M. (2019). Remote sensing for drought monitoring & impact assessment: Progress, past challenges and future opportunities. *Remote Sensing of Environment*, 232, 111291. Retrieved from https://doi.org/10.1016/j.rse.2019.111291

Wilhite, D. A., & Glantz, M. H. (1985). Understanding: The drought phenomenon: The role of definitions. *Water International*, 10(3), 111–120. Retrieved from https://doi.org/10.1080/02508068508686328

WMO. (2016). *Handbook of Drought Indicators and Indices*. *Geneva: World Meteorological Organization (WMO) and Global Water Partnership (GWP)*.

Xu, X., Frey, S. K., Boluwade, A., Erler, A. R., Khader, O., Lapen, D. R., & Sudicky, E. (2019). Evaluation of variability among different precipitation products in the Northern Great Plains. *Journal of Hydrology: Regional Studies*, 24, 100608. Retrieved from https://doi.org/10.1016/j.ejrh.2019.100608

Zaniolo, M., Giuliani, M., Castelletti, A. F., & Pulido-Velazquez, M. (2018). Automatic design of basin-specific drought indexes for highly regulated water systems. *Hydrology and Earth System Sciences*, 22(4), 2409–2424. Retrieved 26 December 2020 from https://doi.org/10.5194/hess-22-2409-2018

Zhang, A., & Jia, G. (2013). Monitoring meteorological drought in semiarid regions using multi-sensor microwave remote sensing data. *Remote Sensing of Environment*, 134, 12–23. Retrieved from https://doi.org/10.1016/j.rse.2013.02.023

6. APPENDIX A: VEGETATION DATA NDVI

For deriving NDVI from MODIS data in GEE, the following background is useful:
The Moderate Resolution Imaging Spectroradiometer (MODIS) provides spectral products, including NDVI, that are widely used for drought assessment and monitoring (West et al., 2019) and can be derived from the Google Earth Engine dataset (GEE) data catalog (Aksoy, Gorucu, & Sertel, 2019). The available vegetation satellite imagery in the Google Earth Engine which is helpful to interpret NDVI in the study area is MODIS (Aqua and Terra), with spatial resolution of 250, 500, and 1000 meters covers the temporal span from the year 2000 to the near real time in a daily temporal resolution (Kumar & Mutanga, 2018).
NDVI is an index that uses red and near-infrared bands and provides information about the vegetation's health and condition by this assumption that healthy vegetation reflects the green bands and contains more water in the signature. This index has often been used for agricultural drought monitoring (Zhang & Jia, 2013).

$$\text{NDVI} = \frac{\text{NIR}-\text{RED}}{\text{NIR}+\text{RED}} \qquad \text{Equation 12}$$

NDVI globally has been accepted as an index to identify agricultural drought in regions with different ecological conditions. It can estimate the best and worst vegetation status over a time scale (Dutta, Kundu, Patel, Saha, & Siddiqui, 2015).
AVHRR and MODIS products have been used to study vegetation conditions, and the 16-days NDVI products from two sensors generate data (Gallo, Ji, Reed, Dwyer, & Eidenshink, 2004). The moderate resolution MODIS has a large swath width and daily revisit intervals (Ogilvie et al., 2015). Drought indices from MODIS satellites also are used in drought monitoring; the sensors with a spatial resolution of 250 m are used to derive NDVI. Spectral products are available in the Google Earth Engine to monitor vegetation health (Kumar & Mutanga, 2018). NDVI equation based on MODIS bands can be derived in equation 12.1 and (McFeeters, 1996) and (Kogan, 1995)

$$\text{NDVI} = \frac{\text{B2} - \text{B1}}{\text{B2} + \text{B1}} \qquad \text{Equation 12.1}$$

As mentioned before, the written codes are available via the respiratory in:
https://github.com/GolnarNaeimi/